SOIL MOISTURE

VISIBLE/INFRARED IMAGER/RADIOMETER SUITE ALGORITHM THEORETICAL BASIS DOCUMENT

Version 3: May 2000

Narinder Chauhan
Liping Di
Shawn Miller
Philip Ardanuy

Steve Running, Science Team Member
University of Montana

RAYTHEON SYSTEMS COMPANY
Information Technology and Scientific Services
4400 Forbes Boulevard
Lanham, MD 20706

SRBS Document #: Y2387

EDR: SOIL MOISTURE

Doc No: Y2387

Version: 3

Revision: 0

	FUNCTION	NAME	SIGNATURE	DATE
Prepared By	EDR Developer	N. CHAUHAN		
Approved By	Relevant IPT Lead	S. MILLER		
Approved By	Chief Scientist	P. ARDANUY		
Released By	Program Manager	H. BLOOM		

TABLE OF CONTENTS

Page

LIST OF FIGURES iii

LIST OF TABLES v

GLOSSARY OF ACRONYMS vi

ABSTRACT vii

1.0 INTRODUCTION 1
- 1.1 HISTORICAL PERSPECTIVE 3
- 1.2 PURPOSE 4
- 1.3 SCOPE 5
- 1.4 VIIRS DOCUMENTS 6
- 1.5 REVISIONS 6

2.0 EXPERIMENT OVERVIEW 7
- 2.1 OBJECTIVES OF SOIL MOISTURE RETRIEVALS 7
- 2.2 INSTRUMENT CHARACTERISTICS 7
- 2.3 RETRIEVAL STRATEGY 7

3.0 ALGORITHM DESCRIPTION 11
- 3.1 PROCESSING OUTLINE 11
- 3.2 ALGORITHM INPUT 13
  - 3.2.1 VIIRS Data 13
  - 3.2.2 Non-VIIRS Data 13
- 3.3 THEORETICAL DESCRIPTION OF SOIL MOISTURE RETRIEVAL 13
  - 3.3.1 Physics of the Problem 13
  - 3.3.2 Mathematical Description of the Algorithm 14
    - 3.3.2.1 Soil Moisture Estimation at CMIS Resolution 14
    - 3.3.2.2 Soil Moisture at VIIRS Resolution 17
  - 3.3.3 Archived Algorithm Output 19
- 3.4 ERROR ANALYSIS AND SENSITIVITY STUDIES 20
  - 3.4.1 Error in Soil Moisture Estimation at the Microwave Resolution 20
    - 3.4.1.1 Microwave Inversion Error (E_{m1}) 21
    - 3.4.1.2 Error due to Data Accuracy and Precision (E_{m2}) 22
  - 3.4.2 Error in Soil Moisture Estimation at High Resolution 23

3.4.3 Calibration Errors 25
3.4.4 Instrument Noise 25
3.4.5 Others 25
3.5 PRACTICAL CONSIDERATIONS 25
3.5.1 Numerical Computation Considerations 25
3.5.2 Programming and Procedural Considerations 25
3.5.3 Configuration of Retrievals 25
3.5.4 Quality Assessment and Diagnostics 25
3.5.5 Exception Handling 26
3.6 ALGORITHM VALIDATION AND DISCUSSION 26
3.6.1 Application to SGP-97 Data 26
3.6.2. Discussion 35
3.6.3 Risks and Risk Reduction Efforts 36
4.0 ASSUMPTIONS AND LIMITATIONS 39
4.1 ASSUMPTIONS 39
4.2 LIMITATIONS 39
5.0 REFERENCES 41
APPENDIX 45

LIST OF FIGURES

Page

Figure 1. An illustration of the importance of soil moisture knowledge from during the 1991 Persian Gulf war. The photo was taken by Associated Press and appeared in *Omaha World Herald* on June 23, 1991. 2

Figure 2. Schematic flow diagram for soil moisture estimation. 12

Figure 3. Schematic representation of the partitioning of microwave radiation from vegetated terrain in terms of the brightness temperature 15

Figure 4. Universal Triangle – Schematic relationship between soil moisture, temperature and NDVI 19

Figure 5. Microwave soil moisture inversion results for four different land surfaces. Dual polarization is used. 22

Figure 6. Location of three sites for the *in situ* soil moisture measurements at the SGP-97 experiment. 27

Figure 7. An example of spatial variability in 0-5 cm soil moisture in a particular field at Little Washita. The variability appears to be consistent for all the four days considered in the present study 28

Figure 8. (a) An example of temporal and spatial variability in 0-5 cm soil moisture measured at the SGP-97 area. Point measurements from each location such as LW are averaged from the data collected from many fields in LW. LW and CF are located at south and north edge of the SGP-97 experimental area. (b) Retrieved surface soil moisture averaged over three locations for June 29-30, July 1-2, 1999. The averaging is done in a 5km x 5km area for a particular location. Note that pixels averaged in (a) and (b) are not identical. 29

Figure 9. High resolution soil moisture plot for the SGP-97 region for 4 days. Soil moisture range varies from 5-20 percent. 31

Figure 10. A plot of microwave (low-resolution) of soil moisture for the SGP-97 area. One-to-one correspondence between Figs. 9 and 10 is observed. 32

Figure 11. Soil moisture map of the SGP-97 area at 1 km resolution. Decreasing trend in soil moisture from June 29 to July 2 is broadly consistent with data. 33

Figure 12. Soil moisture map of the SGP-97 area at 25 km resolution. 34

Figure A1. Schematic representation of the emission model for vegetated terrain based on Peake's approach. 45

Figure A2. Forward model for smooth and rough (s=3 cm l=10cm) surface without vegetation cover. 47

Figure A3. Microwave estimates of soil moisture from bare (rough and flat) surfaces using single polarization and dual-polarization inversion techniques. 49

Figure A4. Illustration of robustness of the soil moisture inversion against noisy data. 49

LIST OF TABLES

Page

Table 1. VIIRS soil moisture EDR requirements *[V-2]*. 4

Table 2. VIIRS spectral bands. 8

Table 3. Soybean canopy parameters 21

Table 4. Error budget for the soil moisture estimation algorithm (%) 24

GLOSSARY OF ACRONYMS

A	Albedo
AMSER	Advanced Microwave Scanning Radiometer
API	Antecedent Precipitation Index
AVHRR	Advanced Very High Resolution Radiometer
CMIS	Conical-Scanning Microwave Imager/Sounder
CrIS	Cross-track Infrared Sounder
DMSP	Defense Meterological Satellite Program
EDR	Environmental Data Record
EOS	Earth Observing System
ESMR	Electronically Scanned Microwave Radiometer
IFOV	Instantaneous Field of View
IPO	Integrated Program Office
IPT	Integrated Product Team
IR	Infrared
LAI	Leaf Area Index
LST	Land Surface Temperature
MODIS	Moderate Resolution Imaging Spectroradiometer
MPDI	Microwave Polarization Difference Index
NDVI	Normalized Difference Vegetation Index
NEDT	Noise Equivalent Temperature Differential
NOAA	National Oceanic and Atmospheric Administration
NPOESS	National Polar-orbiting Environmental Satellite System
POES	Polar Operational Environmental Satellite
RMS	Root Mean Square
SRD	Sensor Requirement Document
SVAT	Soil Vegetation Atmosphere Transfer
SMMR	Scanning Multichannel Microwave Radiometer
SMM/I	Special Sensor Microwave/Imager
SGP-97	Southern Great Plain – 97
USDA	U.S. Department of Agriculture
VIIRS	Visible/Infrared Imager/Radiometer Suite

ABSTRACT

An approach is evaluated for the estimation of soil moisture at high resolution using satellite microwave and optical/infrared (IR) data. This approach is suitable for data that will be acquired by the Visible/Infrared Imager/Radiometer Sensor Suite (VIIRS) and a Conical Scanning Microwave Imager/Sounder (CMIS), planned for launch in 2007-2010 time frame under the National Polar-orbiting Operational Environmental Satellite System (NPOESS). The estimation procedure for soil moisture involves two steps. In the first step, a passive microwave remote sensing technique is employed to estimate soil moisture at low resolution. This involves inversion of dual-polarized microwave brightness temperature using a simple radiative transfer model. In the second step, the microwave-derived low-resolution soil moisture is linked to the scene optical/IR parameters, such as Normalized Difference Vegetation Index (*NDVI*), surface albedo, and Land Surface Temperature (*LST*). The linking of the microwave-derived soil moisture to *NDVI*, surface albedo and *LST* is based on the "Universal Triangle" approach of relating land surface parameters. The three optical/IR parameters are available at high-resolution and are aggregated to the microwave resolution for the purpose of building the linkage model. The linkage model, in conjunction with high-resolution *NDVI*, surface albedo, and *LST*, is then used to disaggregate microwave soil moisture into high-resolution soil moisture.

The technique is applied to data from the Special Sensor Microwave Imager (SSM/I) and Advanced Very High Resolution Radiometer (AVHRR), which were acquired for the duration of the Southern Great Plains (SGP-97) experiment conducted in Oklahoma in June-July 1997. Predicted soil moisture results at higher resolution agree with that of lower resolution results in both magnitude and trend. The spatial patterns and temporal trends in the predicted soil moisture show a reasonable agreement with the *in situ* measurements. An error budget analysis of the soil moisture estimation procedure gives the root mean square (RMS) error less than 5 percent for a typical bare field. The potential of this technique for obtaining an operational, high-resolution, global soil moisture mapping is briefly discussed.

1.0 INTRODUCTION

As a part of its Integrated Program Office (IPO) program, NPOESS will provide an enduring capability to measure, on a global basis, atmospheric, land, and ocean environmental parameters. The system will provide timely and accurate weather and environmental data to weather forecasters, military commanders, civilian leaders, and the scientific community. NPOESS converges the National Oceanic and Atmospheric Administration's (NOAA) Polar Operational Environmental Satellites (POES) and the Defense Department's Defense Meteorological Satellite Program (DMSP) into a single system. NPOESS will operate in near circular, sun-synchronous orbit and is scheduled to fly in the 2007-2010 time frame. A host of satellites with sensors operating in different frequency regions of the electromagnetic spectrum will have equatorial crossings at 0530, 0930, and 1330 local time. The Visible/Infrared Imager Radiometer Suite (VIIRS) and Conical-Scanning Microwave Imager/Sounder (CMIS) will form an important part of NPOESS and will share the same platform. The VIIRS and the CMIS will be successors in technology to the Advanced Very High Resolution Radiometer (AVHRR) and the Special Sensor Microwave/Imager (SSM/I), respectively. There are approximately five dozen parameters to be retrieved from the remote sensing data collected by NPOESS and among them six are considered to be "key" parameters (NPOESS, 1999). The "key" parameters are particularly important to NPOESS mission, and soil moisture is one of the "key" parameters. In this paper, we describe a synergistic optical/IR and microwave approach that could be used by NPOESS for estimating soil moisture at kilometer resolution.

Recent studies have shown the effects of soil moisture on the feedbacks between land-surface and atmospheric processes that lead to climate irregularities (Brubaker and Entekhabi, 1996; Delworth and Manabe, 1989). Simulations have shown that improved characterizations of surface soil moisture and other land surface parameters in numerical weather prediction models can lead to forecast improvement (Beljaars *et al*., 1996). Soil moisture is also an important component of the various processes of the terrestrial ecosystem. It provides a link between the terrestrial surface and the atmosphere through its effects on surface energy and soil moisture fluxes (Sellers *et al*., 1986). Thus, the ability to determine the spatial and temporal distribution of soil moisture would be of significant help in understanding the Earth as an integrated system. Timely information of soil moisture is also used by the military in the efficient planning of their infantry and vehicular traffic in remote areas (Figure 1). NPOESS will provide such a capability on an operational and continuous basis.

Currently, soil moisture product is not available globally. None of the operational missions produce this product. A few surrogates of soil moisture are available—such as soil wetness, flood index, crop index, Antecedent Precipitation Index (API), and others. These surrogates are insufficient substitutes for soil moisture estimates and offer only qualitative information about the soil moisture. Both microwave and optical/IR remote sensing techniques are capable of sensing soil moisture, but the implementation of these sensing techniques from space platform for global soil moisture estimation is lacking. Microwave remote sensing has the potential to provide a direct measure of soil moisture. It also has the advantage of all-weather observations and penetration of vegetation canopy for the soil moisture sensing. However, there are many

Figure 1. An illustration of the importance of soil moisture knowledge from during the 1991 Persian Gulf war. The photo was taken by Associated Press and appeared in *Omaha World Herald* on June 23, 1991.

reasons why microwave techniques have not been applied for the global estimation of soil moisture. First, the resolution of passive microwave sensors from space is poor; second, the available wavelengths from satellites do not provide adequate soil moisture sensitivity for all vegetation covers; third, the *a priori* information that is required in most of the existing soil moisture estimation algorithm cannot be obtained globally. For over a decade , efforts have been made to use longer wavelengths (e.g., L-band) since they provide adequate sensitivity to soil moisture for most of the vegetation cover. However, long wavelengths require large antennas in orbit and are an engineering challenge and the solutions are expensive. The problem scales inversely with frequency and consequently an imaging radiometer at L-band has not been flown in space. In fact, the resolution available for passive microwave remote sensing from space has improved very little from its beginnings with the launch of the Electronically Scanned Microwave Radiometer (ESMR) in 1972. Consequently, despite the success of microwave remote sensing of soil moisture in controlled environments, very little has been done to extend soil moisture remote sensing to global scale. Presently, the microwave sensor technology is not able to provide high-resolution data. Additionally, the microwave algorithms that employ *solely* microwave data are not sufficiently robust to estimate soil moisture without *a priori* information.

1.1 HISTORICAL PERSPECTIVE

A number of techniques that span the whole electromagnetic spectrum have been used to sense soil moisture. However, techniques in the optical/IR and microwave frequency regimes have attracted more attention. Optical/IR sensors provide good spatial resolution and efforts were made in the seventies to use them for soil moisture estimation (Idso *et al.*, 1975; Idso *et al.*, 1976; Price, 1977). Controlled experiments show that the optical/IR approach has the potential to sense soil moisture, but the implementation (particularly from space) has not yet been achieved . Fresh attempts such as those by Cracknell and Xue (1996) are underway for the determination of thermal inertia from space. The returns from optical/IR sensors are equally sensitive to the soil types and it is difficult to decouple the two signatures. In addition, the soil moisture estimates derived from optical/IR sensors require surface micrometeorological and atmospheric information that is not routinely available. These are undoubtedly among the reasons that a soil moisture product has not been slated for future optical/IR missions such as Moderate Resolution Imaging Spectroradiometer (MODIS).

Passive microwave remote sensing has been used widely to provide a quantitative, direct estimate of soil moisture (Njoku and Li, 1999; Jackson *et al*., 1982; Engman, 1991). The soil moisture maps obtained in Southern Great Plains experiment (SGP-97), Washita-92, Moonsoon-90 and First ISLSCP Field Experiment (FIFE) were all provided by the passive sensors operating at L-band. In most cases, a simple radiative transfer model is inverted to obtain Fresnel reflectivity. *A priori* information of vegetation optical depth and RMS height, is used to estimate soil moisture (Jackson and LeVine, 1996). Given the spatial resolution and frequency, the current generation of spaceborne microwave radiometers is not optimal for land remote sensing. SSM/I launched in 1987 has the lowest frequency of 19.4 GHz and a spatial resolution of ~56 km. The Scanning Multichannel Microwave Radiometer (SMMR) launched on the Nimbus-7 satellite in 1978, had a spatial resolution of ~150 km at its lowest frequency of 6.6 GHz. Lower frequencies such as L-band are preferred for soil moisture since they provide adequate sensitivity to soil moisture for most of the vegetation cover. However, because of practical problems of supporting a large, low-frequency antenna in space, the prospect of having a spaceborne low-frequency microwave sensor remains remote.

Attempts have been made to use microwave satellite data for the soil moisture estimation. Van de Griend and Owe (1993) and Owe *et al*. (1992) have written a series of papers on the characterization of soil moisture and vegetation properties from SMMR data over Southern Africa. They also presented empirical relationships between vegetation optical depth and optical parameters such as Normalized Difference Vegetation Index (NDVI*)*. Such relationships have not been confirmed independently. Jackson (1997) used SSM/I data at 19.4 GHz together with *a priori* values of single scattering albedo and optical depth, to estimate soil moisture for a grass-dominated subhumid area near Oklahoma. He concluded that his approach could not be used for soil moisture estimation from other vegetation canopies. In a recent paper, Njoku and Li (1999) have demonstrated an estimation approach that could be used to derive soil moisture from Advanced Microwave Scanning Radiometer (AMSR) scheduled to fly on Earth Observing System (EOS) PM-1 platform in 2000. The lowest frequency on AMSER will be 6.9 GHz and the footprint size of 43 km x 75 km. The microwave equivalent of thermal inertia, known as radiobrightness thermal inertia, has also been used to estimate soil moisture from satellite microwave data for the controlled experiments (England *et al*., 1992).

1.2 PURPOSE

This document summarizes the theoretical basis, development process, and functional flow of the Visible/Infrared Imager/Radiometer Suite (VIIRS) soil moisture Environmental Data Record (EDR) estimation process. The document is evolutionary in nature and will undergo periodic changes to fulfill threshold requirements and some objectives given in the VIIRS Sensor Requirement Documents (SRD) *[V-1]* and *[V-2]*.

In our original proposal, soil moisture was identified as a high-risk EDR . Employing an approach outlined in this document, the risk has been reduced considerably, and partial objectives have been achieved. This document identifies sources of input data (both VIIRS and non-VIIRS) that are required for the soil moisture retrieval. It provides theory and mathematical background underlying the use of this information in the retrieval process. The implementation, assumptions, and limitations of the adopted approach are also discussed in this document. Some results and validation of the algorithm are also discussed. The main purpose is to provide a sound, repeatable, step-by-step approach for estimating soil moisture within the limits defined in the VIIRS Sensor Requirement Document (SRD). The VIIRS SRD *[V-1]* requirements are shown in Table 1.

Table 1. VIIRS soil moisture EDR requirements *[V-2]*.

Para. No.	Parameter	Threshold	Objective
V40.2.6-1 V40.2.6-2	a. Horizontal Cell Size 1. Clear, at nadir (TBR) 2. Clear, worst case (TBR) 3. Cloudy, at nadir 4. Cloudy, worst case	 1 km 4 km 40 km 50 km	 (TBD) 2 km 2 km (TBD)
V40.2.6-3	b. Horizontal Reporting Interval	(TBD)	(TBD)
V40.2.6-4	c. Vertical Cell Size	0.1 cm	5 cm
V40.2.6-5	d. Vertical Reporting Interval	N/A	5 cm
V40.2.6-6	e. Horizontal Coverage (TBR)	Land	Land
V40.2.6-7	f. Vertical Coverage	Surface to –0.1cm (skin layer)	Surface to –80cm
V40.2.6-8	g. Measurement Range	0-100 cm/m (TBR)	0-100 cm/m
V40.2.6-9	h. Measurement Uncertainty 1. Clear, bare soil in regions with known soil types (smaller horizontal cell size) 2. Cloudy, bare soil in regions with known soil types (greater horizontal cell size)	 10 cm/m (TBR) 20 cm/m (TBR)	 Surface: 1cm/m Surface: 1cm/m
V40.2.6-10	i. Mapping Uncertainty	3 km	1 km
	j. Maximum Local Average Revisit Time	8 hrs	3 hrs
	k. Maximum Local Refresh	(TBD)	(TBD)
V40.2.6-11	l. Minimum Swath Width	3000 km (TBR)	(TBR)

Units: cm/meter (cm of water per meter of soil depth)

1.3 SCOPE

To achieve accuracy and high spatial resolution, it seems natural to have a technique that combines the strengths of microwave as well as optical/IR remote sensing approaches for the soil moisture estimation. This document describes a two-step approach to obtain operational, reasonably accurate, high-resolution soil moisture by linking microwave-derived soil moisture estimates with optical/IR parameters. First, the soil moisture at low resolution is retrieved from microwave data. The microwave estimates are limited to weakly vegetated terrain to ensure the accuracy of the retrieved soil moisture. We use both the horizontal and vertical polarizations at the lowest available radiometer frequency and invert the ratio of horizontal to vertical Fresnel reflectivity to obtain soil moisture. It is widely believed that the proposed design of CMIS will have a C-band along with other high frequency channels. The technique is suitable for satellite remote sensing and does not require *a priori* information. Secondly, to increase resolution, relationships are derived between microwave-derived soil moisture, NDVI, surface albedo, and Land Surface Temperature (LST). The latter three parameters are obtained from satellite data acquired by a high-resolution optical/IR sensor and aggregated to the microwave resolution for the purpose of building relationships. The model is then applied backwards to high-resolution NDVI, surface albedo, and LST to obtain high-resolution soil moisture. The final soil moisture estimates are greatly improved in terms of spatial resolution and accuracy in comparison to the soil wetness product currently produced by NOAA. The enhancement of spatial resolution of soil moisture from ~50 km to ~1 km, is a highly relevant research development in this area.

An error and sensitivity analysis has been performed on the estimation procedure. For the microwave part, error analysis is carried out using an emission model that is robust and has been validated for a variety of canopy covers. For the high-resolution estimation, error analysis is performed using SSM/I and AVHRR data. Finally, the soil moisture estimation technique is applied to Southern Great Plain – 97 (SGP-97) data that was collected in Oklahoma. *In situ* soil moisture (0-5 cm deep) collected during the SGP-97 experiment is compared against the predictions. The limitation of point measurements for validation of soil moisture maps is also discussed.

This document covers the algorithm theoretical basis for the soil moisture EDR that is to be routinely retrieved. It discusses the unique capability of the National Polar-orbiting Environmental Satellite System (NPOESS) sensors (VIIRS, and the Conical-Scanning Microwave Imager Sounder [CMIS]) to estimate soil moisture on regional and global scales. The threshold requirement is to estimate soil moisture from bare soil and the objective requirement is to estimate soil moisture from any surface including moisture profiles with depth. Section 3 discusses the rationale for the development of the soil moisture estimation algorithm and includes mathematical descriptions, sensitivity studies, and practical considerations for the implementation of the retrieval algorithm. The results and the validation of the algorithm presented here are focused toward achieving the threshold requirement.

The Raytheon soil moisture Integrated Product Team (IPT) has developed a new algorithm to produce the global soil moisture EDR. The microwave estimation of soil moisture is much improved from the existing (soil wetness) product produced for operational purposes. The extension of microwave resolution from 50 km to 1 km is a new research development. This new technique/algorithm is being written in the form of a research paper and will be submitted for publication (Chauhan *et al.*, 1999).

1.4 VIIRS DOCUMENTS

Reference to VIIRS documents is indicated by a number in brackets, e.g., *[V-1]*.

[V-1] NPOESS IPO, 1997, Visible/Infrared Imager/Radiometer Suite (VIIRS), Sensor Requirement Document (SRD), Prepared by Associate Directorate for Acquisition, NPOESS Integrated Program Office.

[V-2] NPOESS IPO, 1998, Visible/Infrared Imager/Radiometer Suite (VIIRS), Sensor Requirement Document (SRD), Prepared by Associate Directorate for Acquisition, Revision 1, NPOESS Integrated Program Office.

[V-3] NPOESS IPO, 1999, Technical Requirement Document (TRD), Appendix D. Prepared by Associate Directorate for Acquisition, NPOESS Integrated Program Office.

[C-1] NPOESS IPO, 1997, Conical-scanning Microwave Imager Sounder (CMIS), Sensor Requirement Document (SRD), Prepared by Associate Directorate for Acquisition, NPOESS Integrated Program Office.

1.5 REVISIONS

The original version of the document was dated July 30, 1998. Revision 1 is dated September 1998. Revision 2 was dated June 1999. Revision 3 is dated May 2000.

2.0 EXPERIMENT OVERVIEW

2.1 OBJECTIVES OF SOIL MOISTURE RETRIEVALS

The NPOESS VIIRS SRD defines threshold requirements as well as objectives of the soil moisture retrieval. Under clear conditions, the threshold requirement is to measure soil moisture only within a thin layer at the surface (0.1 cm thick) and only for bare soil in the region of known soil types. The objective is to measure a moisture profile up to a depth of 80 cm below the surface for any soil, whether bare or not, and whether or not the soil type is known. Soil moisture EDR is a 1 km global daily product under clear sky conditions with measurement uncertainty not to exceed 10 percent. For estimation under cloudy conditions, the horizontal cell size is 40 km and uncertainty not to exceed 20 percent. The uncertainty in the objectives should not exceed 1 percent in the surface soil moisture estimates and 5 percent in profile estimation. The threshold requirement for minimum swath width is 3,000 km. The details are given in Table 1.

2.2 INSTRUMENT CHARACTERISTICS

The VIIRS sensor will provide global coverage with a 16-day repeat cycle at the equator and a 3-day repeat cycle at the poles. It will fly in an 833 km descending orbit with an equatorial crossing time of 9:30 AM. The VIIRS sensor is a cross-track sensor with the spectral channels listed in Table 2 arranged on three focal planes. The minimum swath width is 1700 km. The nadir pixel size is approximately 375 m for the imagery resolution bands (5i, 6i, 8i, 10iw, and 12iw) and 750 m for the moderate resolution bands.

2.3 RETRIEVAL STRATEGY

The optical sensors are reasonably good in sensing soil moisture but are also equally sensitive to soil types. It is difficult to decouple the two signatures. This perhaps is one of the reasons that a soil moisture product has not been attempted from the Moderate Resolution Imaging Spectroradiometer (MODIS). However, VIIRS has an advantage over MODIS due to the inclusion of a passive microwave sensor CMIS on its platform. Our retrieval strategy takes advantage of the presence of these two sensors on the same platform. The estimation algorithm uses synergistically collected microwave-optical data for the estimating soil moisture. The microwave sensors are relatively insensitive to soil types but can give quantitative estimates of soil moisture when used in conjunction with optical/thermal sensors. This document discusses the combined use of optical and microwave data to estimate soil moisture. Because microwave data will be available at much lower resolution than optical data, the traditional soil moisture estimation algorithm using synergistic microwave and thermal data will be extended to generate a high resolution, 1 km soil moisture EDR.

Table 2. VIIRS spectral bands.

VIIRS BAND	Center (μm)	Width (μm)	Nadir pixel size (m)
Chlor2	0.412	0.020	750
2	0.445	0.018	750
Chlor8	0.488	0.020	750
4	0.555	0.020	750
5i	0.645	0.050	375
OC2	0.672	0.020	750
OC3	0.751	0.015	750
6i	0.865	0.039	375
6r	0.865	0.039	750
Cloud1	1.240	0.020	750
7	1.378	0.015	750
8i	1.610	0.060	375
8r	1.610	0.060	750
9	2.250	0.050	750
10r	3.700	0.180	750
10iw	3.740	0.380	375
SST2	4.050	0.155	750
SST4	8.550	0.300	750
11	10.783	1.000	750
12iw	11.450	1.900	375
12r	12.013	0.950	750
DNB	0.700	0.400	750

Implementation of the combined optical-microwave algorithm involves the following steps:

- Estimate soil moisture at CMIS resolution using CMIS-derived microwave brightness temperature, VIIRS-derived aggregated Land Surface Temperature (LST), and Normalized Difference Vegetation Index (NDVI).
- Because soil moisture is related to NDVI, LST, and surface albedo (A), develop regression relations between microwave-derived soil moisture and aggregated VIIRS-derived NDVI, LST, and A.
- Use the regression coefficients, VIIRS-derived non-aggregated km-scale NDVI, LST, and A to obtain soil moisture EDR at 1 km resolution.

A parallel effort is also under way by the CMIS group/contractor to estimate soil moisture EDR at CMIS resolution. Most of the requirements, such as measurement uncertainty and vertical coverage, are the same for VIIRS and CMIS for the soil moisture EDR even though horizontal cell sizes are different for the two sensors. The horizontal cell size and minimum swath width for VIIRS are 1 km and 3,000 km, while for CMIS these are 40 km and 1700 km, respectively. At the present stage of the VIIRS contract, we are insulated from CMIS activities; therefore, we decided to develop our own state-of-the-art microwave algorithm for soil moisture estimation from CMIS data. This includes a forward model to simulate CMIS data (microwave brightness temperature). This will allow us to meet the measurement uncertainty requirement given in *[V-2]*.

For cloudy conditions, soil moisture threshold requirements for resolution and measurement uncertainty are the same for VIIRS and CMIS. Therefore, we have decided not to duplicate the CMIS effort.

3.0 ALGORITHM DESCRIPTION

3.1 PROCESSING OUTLINE

The VIIRS soil moisture retrieval approach involves inversion of CMIS data using a simple radiative transfer model to obtain microwave surface reflectivity. The microwave surface reflectivity is converted to obtain soil moisture. At this stage the soil moisture product is at CMIS resolution. The resolution of this product is improved by regressing soil moisture against NDVI, albedo, and LST, which are available at roughly 1 km resolution (Chauhan *et al.*, 1999). Figure 2 depicts the processing concept for soil moisture retrieval over bare and weakly vegetated surfaces.

The retrieval process is assisted by the availability of two VIIRS-derived EDRs. The first EDR, NDVI, is used to distinguish between vegetated and nonvegetated areas. It is also used to quantify vegetation, so as to limit the application of the soil moisture estimation algorithm to a certain level of vegetation where the microwave soil moisture estimation algorithm will be valid. Note that the threshold requirement is to estimate soil moisture only for bare soil. The second EDR, LST, is used to scale microwave brightness temperature to obtain the microwave emissivity of the soil surface. Aggregated NDVI, LST, and surface albedo are used in the microwave inversion process, while for VIIRS soil moisture EDR estimation, nonaggregated (1 km) NDVI, LST, and surface albedo are used.

Soil moisture estimation under vegetation is still a topic of research, and there is no single acceptable algorithm to predict soil moisture from vegetated areas. Therefore, the present algorithm will only be applied to weakly vegetated areas, such as grassland and short agricultural crops. NDVI will be used to limit the vegetation pixels.

As is clear from the outline given in Figure 2, the core of the process in the current soil moisture determination involves a synergistic analysis of microwave-optical/infrared data. The algorithm combines the traditional accuracy of microwave sensors for soil moisture sensing with the high-resolution capability of the optical/infrared sensors to determine a soil moisture estimate at 1 km resolution. This ATBD describes the second version of this algorithm, and will require more fine-tuning as we move along.

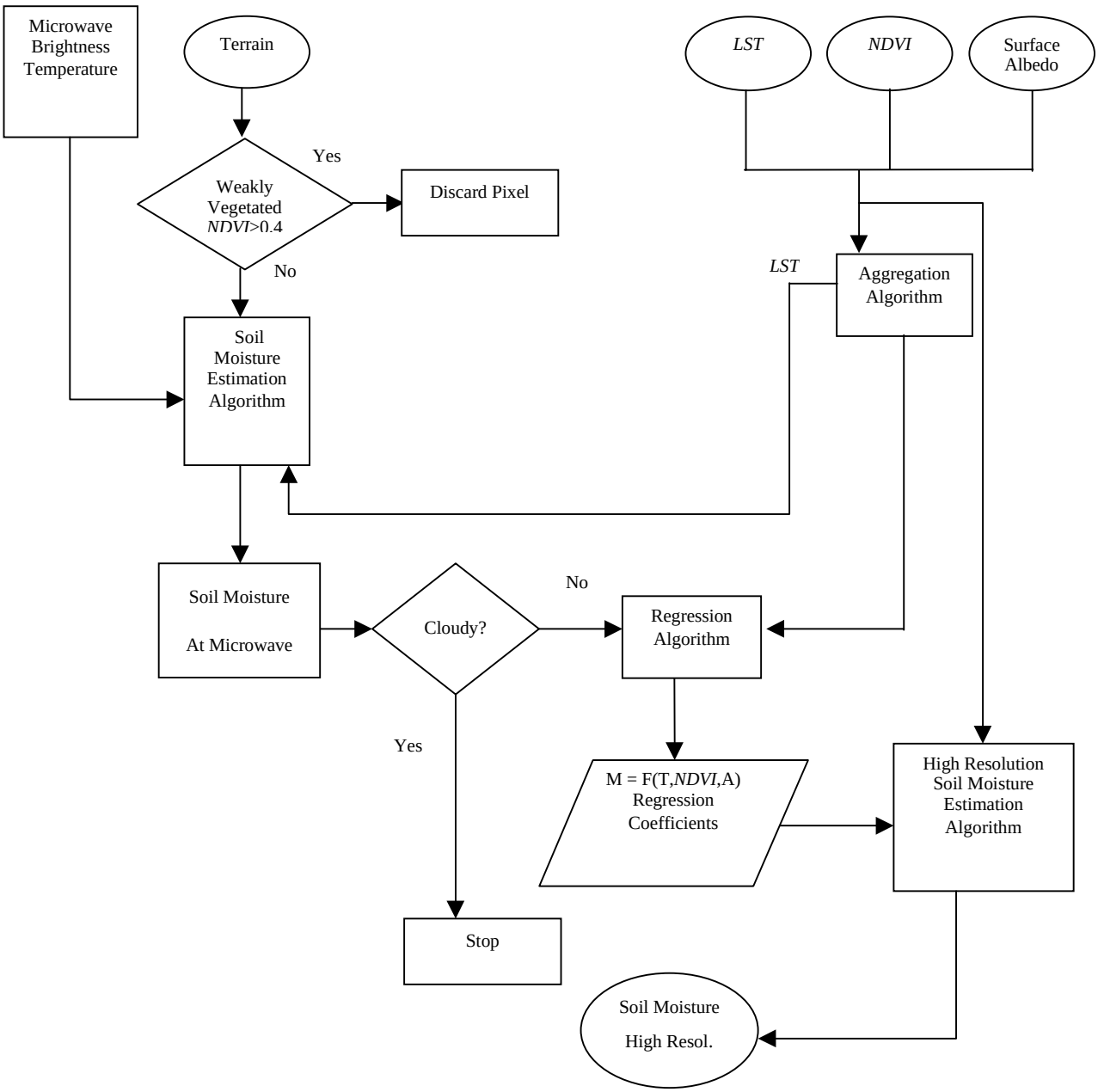

Figure 2. Schematic flow diagram for soil moisture estimation.

3.2 ALGORITHM INPUT

3.2.1 VIIRS Data

VIIRS-produced EDRs (i.e., NDVI, LST, and surface albedo) are required in the soil moisture estimation algorithm. NDVI is used to separate vegetated and nonvegetated areas. It is also used to quantify the vegetation amount.

3.2.2 Non-VIIRS Data

The algorithm requires synergistic microwave brightness temperatures from CMIS at both horizontal and vertical polarization [*C-1*] at the lowest CMIS frequency. In addition, a data bank of rivers, lakes, streams, other water bodies; an ocean/land mask; and a cloud mask are also needed.

3.3 THEORETICAL DESCRIPTION OF SOIL MOISTURE RETRIEVAL

3.3.1 Physics of the Problem

The soil moisture estimation algorithm consists of two steps. Step One involves soil moisture estimation at CMIS resolution using CMIS microwave brightness temperature and aggregated LST. Step Two deals with improving the resolution of soil moisture (estimated in the first step) by incorporating nonaggregated km-scale LST, NDVI, and albedo EDRs. This produces a soil moisture EDR product at 1 km scale resolution. Both steps are based on well known physics.

The theoretical basis for measuring soil moisture in Step One is based on the large contrast between the dielectric properties of water and dry soil. The large dielectric constant for water is the result of the water molecule alignment of the dielectric dipole in response to the applied electromagnetic field. For example, at C-band the real part of the dielectric constant of water is about 80 compared to that of dry soil, which is on the order of 3-5. Thus, as the soil moisture increases, the dielectric constant of the soil increases, and this change is detected by microwave sensors. It is interesting to note that the dielectric constant has a weak dependence on soil types. As a result, microwave remote sensing techniques for soil moisture estimation do not require precise knowledge of soil types.

Soil moisture estimation at the microwave resolution employs microwave brightness temperature and aggregated *LST*. The retrieval is performed using a radiative transfer model. Because most of the remote sensing problems are ill-posed, a straightforward inversion of radiative transfer models is complicated. The retrieval model is a simplified version of the rigorous model described by Tsang *et al*. (1985), but it contains most of the essential elements that are required for soil moisture estimation. The microwave algorithm is limited to weakly vegetated areas. In the present paper, the algorithm is applied to pixels with NDVI ≤ 0.4. This condition, however, depends on the channel frequency of the microwave data. The accuracy of the microwave algorithm for the soil moisture estimation in vegetated areas degrades with increased channel frequency.

The second step involves developing a relationship between the microwave-derived soil moisture and NDVI, temperature, and albedo. It is well known that the surface radiant temperature of bare soil illuminated by sunlight is highly correlated with soil wetness (Idso *et al.*, 1975). The spatial

variations of the radiant temperature are highly dependent on the fraction of bare soil viewed by the radiometer and surface soil water contents. Vegetation, however, complicates the problem. A rigorous way to understand these relationships is through the modeling of the Soil Vegetation Atmosphere Transfer (SVAT) of energy using an energy budget approach. However, Carlson *et al.* (1994) and Gillies *et al.* (1997) were able to generate a simple regression relation among the three parameters (NDVI, soil moisture, and soil temperature) by careful analyses of available data. The results were later confirmed by the University of Pennsylvania SVAT model. A unique relationship between the surface soil moisture availability and the radiant temperature does not exist in the presence of vegetation cover, but relative variations in NDVI and temperature show a fairly stable relationship to soil moisture availability over a wide range of climatic conditions and land surface types (Carlson *et al.*, 1994). Therefore, the second step of the soil moisture estimation process is to determine relationship between microwave-derived soil moisture, *NDVI*, temperature, and albedo through regression - a practice established by Carlson *et al*. (1994). These regression relations, in conjunction with high resolution NDVI, LST, and albedo, are then used to obtain soil moisture at high resolution.

Figure 2 illustrates the soil moisture estimation algorithm. The details of these steps are described in the following sections.

3.3.2 Mathematical Description of the Algorithm

The algorithm to retrieve soil moisture from microwave data is described first. Instead of presenting the complicated details of the transport theory, a simplified version of the retrieval model that is based on radiative transfer theory is described in the following section. The next section focuses on the regression model used in the inversion process and skips the complicated derivation of the model from SVAT theory.

3.3.2.1 Soil Moisture Estimation at CMIS Resolution

A layer of vegetation over soil attenuates emission from the soil and adds to the radiative flux with its own emission. A simple radiative transfer model describing the brightness temperature of a weakly scattering vegetation layer above a semi-infinite medium was first developed by Basharinov and Shutko (1975) and is described in Ulaby *et al.* (1982). A schematic representation of the partitioning of microwave radiation from a vegetated surface in terms of the brightness temperature T_B is shown in Figure 3. Mathematically, T_B can be written as:

$$T_B = T_s(1-R_s)e^{-\tau} + (1-\omega)T_v(1-e^{-\tau}) + R_s(1-\omega)T_v(1-e^{-\tau})e^{-\tau} \quad (1)$$

where T_s and T_v are soil and vegetation temperatures respectively, R_s is the reflectivity of the soil surface, τ is the vegetation optical depth, and ω is the single-scattering albedo of vegetation. In the above equation $(1-R_s)$ is defined as emissivity and $e^{-\tau}$ is called canopy attenuation. The polarization dependence in Equation 1 has been suppressed for the sake of simplicity.

The three terms in Equation 1 represent dominant contribution to microwave emission from a typical land surface. The first term is the radiation emitted by the soil surface multiplied by the canopy transmissivity. The second term is the upward radiation from vegetation, and the last term is the downward radiation from vegetation reflected at the soil surface and attenuated by vegetation. As can be seen in Equation 1, the soil moisture effects on emission are from the first

and third terms in the form of surface reflectivity R_s.

Equation 1 assumes that the atmospheric and sky contributions to T_B are small and are ignored here. Microwave brightness temperatures from space are modified by atmosphere. Short-term comparisons of T_B are generally valid at low frequencies. Over longer periods (seasonal or yearly) however, atmosphere must be taken into account. As noted by Choudhury (1993), the magnitude of the effect of atmosphere at mid-latitudes at 19 GHz is of the order of +3K. CMIS frequency used in the present soil moisture retrieval process will probably be lower than 19 GHz. As a result, atmospheric contribution to brightness temperature will be small and is not accounted for here.

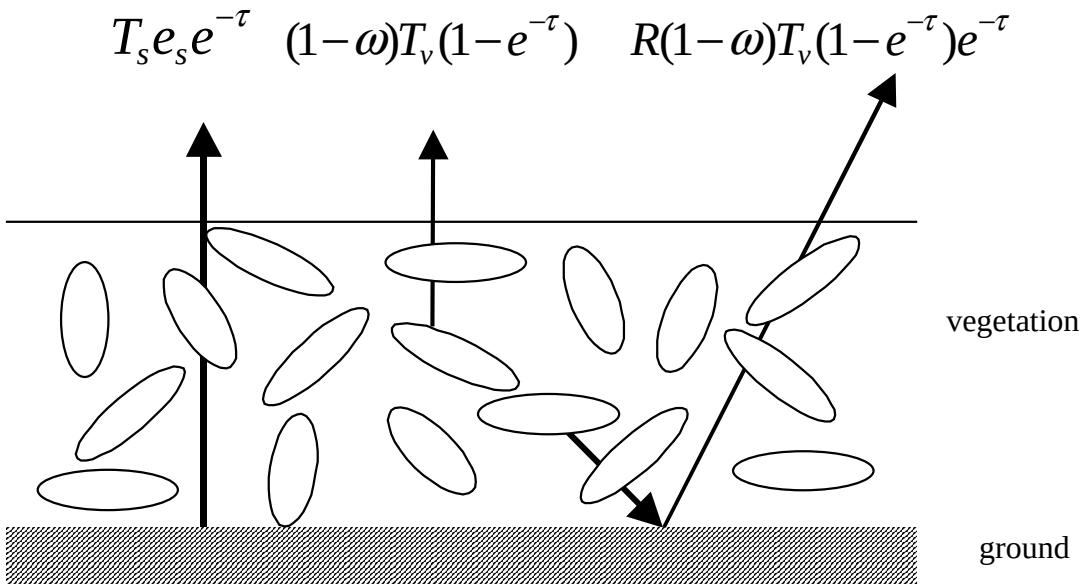

Figure 3. Schematic representation of the partitioning of microwave radiation from vegetated terrain in terms of the brightness temperature.

For most non-forest vegetation, $T_s \sim T_v = T$. Equation 1 then reduces to:

$$T_B = T\left\{(1-R_s)e^{-\tau} + (1+R_s e^{-\tau})(1-\omega)(1-e^{-\tau})\right\} \tag{2}$$

If the vegetation is considered as a purely absorbing medium such that the single-scattering albedo is negligibly small, then Equation 2 reduces to:

$$T_B = T\left[1 - R_s e^{-2\tau}\right] \tag{3}$$

The reflectivity R_s depends on the soil dielectric constant and is related to soil moisture (Hallikainen *et al.*, 1985). If the ground surface is rough, the reflectivity is modified by the surface roughness and is given by

$$R_s = \left|R_g\right|^2 e^{-4k_o^2 s^2 \cos^2\theta_i} \tag{4}$$

Here, s is the RMS height of the rough surface, k_o is the free space wave number, θ_i is the view angle of the radiometer, and $\left|R_g\right|^2$ is the Fresnel reflectivity of the soil.

To obtain soil moisture, Equation 3 is inverted and surface reflectivity is determined first. Most of the past studies (Jackson *et al*., 1982; Chauhan, 1997; O'Neill, 1996) have used the horizontally polarized microwave brightness temperature for soil moisture estimation because of Brewster angle effects in the vertically polarized data. To invert Equation 3, both the surface RMS height s and optical depth τ are required. It is important to note that both of these parameters appear in the exponential and consequently, they need to be known very accurately. Small inaccuracies in their estimation will rapidly swamp the soil moisture estimation accuracy (Chauhan, 1999a). Furthermore, these parameters are difficult to estimate, especially from a space platform.

We have followed a two-polarization technique that can be applied for the estimation of soil moisture from a space platform. The technique is an improvement over the existing single-polarization technique, as neither the surface RMS height nor the optical depth is required in the algorithm for the soil moisture estimation. The microwave frequencies from the space platform can penetrate only weak vegetation, therefore, the microwave algorithm is limited to pixels having NDVI less than or equal to 0.4. This condition will change if a lower microwave frequency is available from the satellite. An examination of the expression of rough surface reflectivity in Equation 4 reveals that the exponential part is polarization independent. Therefore, a ratio of horizontal to vertical reflectivity is independent of surface RMS height, and as a result, the surface roughness effects are eliminated through the ratio. Equation 3 is rewritten as:

$$\frac{\left|R_g^h\right|^2}{\left|R_g^v\right|^2} = \left\{\frac{T - T_{Bh}}{T - T_{Bv}}\right\} e^{2(\tau_h - \tau_v)} \tag{5}$$

In Equation 5, T_{Bh}, $\left|R_g^h\right|^2$, and T_{Bv}, $\left|R_g^v\right|^2$ are brightness temperatures and Fresnel reflectivities, for horizontal and vertical polarization, respectively. At the microwave frequencies available for the current spaceborne sensors, the horizontal and vertical optical depths for vegetation are close to one another and more so for weak vegetation such as short agricultural crops and grasslands (Chauhan, 1999a). As a result, $\tau_h - \tau_v \cong 0$. Since temperatures can be determined from the satellite data, the ratio of the Fresnel reflectivities can be calculated from Equation 5.

To obtain soil moisture from Equation 5, the real part of the dielectric constant is expressed using the analytical expression of horizontal (R_g^h) and vertical (R_g^v) Fresnel reflection coefficients as:

$$\varepsilon_g = \left(\frac{1-R_g^h}{1+R_g^v}\right)\left(\frac{1-R_g^v}{1+R_g^h}\right) \tag{6}$$

The dielectric constant obtained from above is converted to soil moisture using the relations given by Hallekainen *et al*. (1985). In the present investigation, the equations above are used to obtain coarse-resolution soil moisture from land surfaces.

Estimation of vegetation characteristics

If dual polarizations are not available on CMIS (a highly unlikely sceranio), then horizontally polarized microwave brightness temperature can be inverted to obtain soil moisture. Equation 2 is invertable for vegetated surfaces (Chauhan, 1997; O'Neill *et al.*, 1996), provided the estimates of ω and τ are known for different vegetation covers. One approach is to classify vegetated areas into 6 biomes (Myneni *et al.*, 1997) and generate look-up tables for optical depth and single-scattering albedo for the six biomes. Because LAI is the driving variable and will be available as a VIIRS by-product parameter for the six biomes, both ω and τ can be calculated as a function of LAI for different biomes. The discrete scatter model by Chauhan *et al.* (1994) can be used to generate look-up tables. The accuracy of this treatment depends on ω and τ, and the model used in the inversion process. As the sensor frequency goes higher or if LAI is high, Equation 2 becomes less accurate. Furthermore, this approach requires frequent refreshing of LAI estimates throughout the year and they may or may not be available.

Alternatively, a simple operationally based treatment has been found to give reasonable soil moisture results for vegetated areas using SMMR frequency = 6.6 GHz satellite data. It is assumed for grassland and savanna types of vegetation that the single-scattering albedo is negligibly small, so that Equation 3 can be used for soil moisture estimation. For SMMR data, the transmissivity $\gamma = e^{-\tau}$ has been found to be related to NDVI (Van de Griend and Owe, 1993) such that:

$$\gamma = e^{-\tau} = 0.7049 - 0.6141 * NDVI \tag{7}$$

Similar corrections for vegetation have also been proposed using a microwave Polarization Index (Paloscia and Pampaloni, 1988) and its surrogate, such as a Microwave Polarization Difference Index (MPDI). Note that the contribution of sky radiation to the microwave brightness temperature T_B has been ignored here, and the vegetation is assumed to be short/sparse enough so as not to contribute to a significant emission of its own, i.e., the scattering albedo is negligibly small. Also, caution must be excerised because the empirical relations, such as those in Equation 11, have not been confirmed independently.

3.3.2.2 Soil Moisture at VIIRS Resolution

Soil moisture coupling to land-surface interactions has been used in the past to quantify soil moisture signatures. NDVI and soil temperature are proven indicators of the vegetative and thermal state of the land surface. However, the vegetation and soil temperature have a complicated dependence on soil moisture. Careful analyses of data by Carlson *et al.*, (1994) and Gillies *et al.*, (1997) have shown that there can be a unique relationship among soil moisture,

NDVI, and soil temperature for a particular region. The results were validated using data analyzed from three experiments conducted at Mahantango, Kansas and in Costa Rica (Carlson *et al.*, 1994). In addition, such relationships are also confirmed by theoretical studies using a soil-vegetation-atmosphere-transfer (SVAT) model. A similar technique has also been used by Nemani *et al*. (1993) to determine surface moisture status from satellite data.

Figure 4 represents a schematic description of the relationship, sometimes referred to as the "universal triangle". Here, soil moisture varies from right (low value) to left (high value) in the triangle. The abscissa and the ordinate are scaled versions of temperature and NDVI respectively such that:

$$T^* = \frac{T - T_o}{T_s - T_o} \tag{8}$$

$$NDVI^* = \frac{NDVI - NDVI_o}{NDVI_s - NDVI_o} \tag{9}$$

where T and NDVI are observed soil temperature and NDVI respectively, and the subscripts o and s stand for minimum and maximum values. Carlson *et al.* (1994) found that the relationship between soil moisture M, $NDVI^*$, and T^* can be expressed through a regression formula such as:

$$\begin{aligned} M = {} & a_{00} + a_{10}NDVI^* + a_{20}NDVI^{*2} \\ & + a_{01}T^* + a_{02}T^{*2} \\ & + a_{11}NDVI^*T^* + a_{22}NDVI^{*2}T^{*2} \\ & + a_{12}NDVI^*T^{*2} + a_{21}NDVI^{*2}T^* \end{aligned} \tag{10}$$

In terms of regression coefficients a_{ij}, Equation (10) can be written as:

$$M = \sum_{i=0}^{i=2}\sum_{j=0}^{j=2} a_{ij} NDVI^{*(i)} T^{*(j)} \tag{11}$$

Carlson (1998) claimed that a single polynomial such as the one above represents a wide range of surface climate conditions and land surface types. The second or third order polynomial gives a reasonable representation of the data.

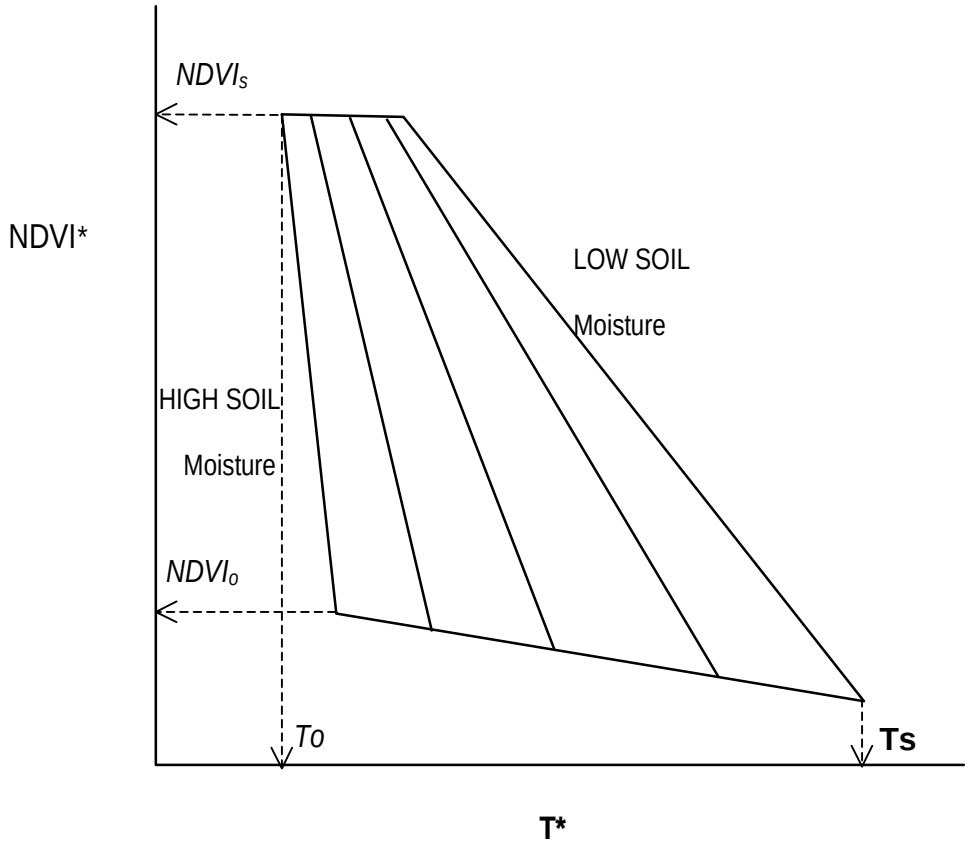

Figure 4. Universal Triangle – Schematic relationship between soil moisture, temperature and NDVI

To apply Carlson's "universal triangle"concept in the present context, the left-hand side in (11) is replaced by microwave-derived soil moisture. In addition to NDVI and LST on the right-hand side of Equation 11, surface albedo (*A*) is added to strengthen the relationship between soil moisture and measurable land parameters. A correct combination of NDVI and A can be useful in representing high-end soil moisture. Therefore, Equation 11 is modified to:

$$M = \sum_{i=0}^{i=2}\sum_{j=0}^{j=2}\sum_{k=0}^{k=2} a_{i\ jk} NDVI^{*(i)} T^{*(j)} A^{*(k)} \tag{12}$$

where

$$A^* = \frac{A - A_o}{A_s - A_o} \tag{13}$$

3.3.3 Archived Algorithm Output

Volumetric soil moisture EDR at VIIRS pixel resolution, along with some flags indicating quality of the retrieved parameter will be archived directly as a final product.

3.4 ERROR ANALYSIS AND SENSITIVITY STUDIES

An error analysis of the soil moisture estimation procedure has been performed to calculate the total error budget. The total error is broken down into respective errors in the low-resolution (microwave) and high-resolution (optical/IR) parts of the algorithm. Errors from each of these parts have been further subdivided for error budget calculation. The following definitions of accuracy, precision and uncertainty are given to understand different errors in the error budget for the soil moisture estimation.

The measurement accuracy A is defined as;

$$A = |\mu - T| \tag{14}$$

where

$$\mu = \frac{1}{N}\sum_{i=1}^{N} X_i \tag{15}$$

and μ is the average of all the measured values X_i corresponds to a true value T. The precision P, as defined in the SRD, is the standard deviation of the measurements from their average value and is expressed as:

$$P = \sqrt{\frac{1}{N-1}\sum_{i=1}^{N}(X_i - \mu)^2} \tag{16}$$

Finally, the uncertainty is defined as:

$$U = \sqrt{\frac{1}{N}\sum_{i=1}^{N}(X_i - T)^2} \tag{17}$$

From the above definition, one can write

$$U = \sqrt{A^2 + P^2} \tag{18}$$

Thus, the uncertainty equals the RMS error between the measurements X_i and the true value T. It is important to note here that precision and accuracy are quite different yardsticks for characterizing data quality. Based on these definitions, the calibration errors can be lumped into accuracy error.

3.4.1 Error in Soil Moisture Estimation at the Microwave Resolution

The error at the microwave resolution is composed of two separate errors. The first error is the microwave algorithm error and is due to the inversion procedure employed to retrieve soil moisture from the microwave data. The second error is contributed by the data accuracy and precision.

3.4.1.1 Microwave Inversion Error (E_{m1})

As described in Section 3.3.2.1, a radiative transfer model is used to invert dual-polarized microwave brightness temperature. To estimate error in this procedure, we have generated microwave brightness temperature data for four different types of land surfaces using Peake's approach (Peake, 1959). The emission model is based on a discrete scatter model and has been used extensively in the forward modeling of agricultural crops (Chauhan *et al*., 1994), Grassland (Saatchi *et al*., 1994) and forest canopies (Chauhan *et al*., 1999b). A brief description of the emission model is given in the Appendix. The four surfaces used in the modeling are; bare smooth, bare low roughness (s=1 cm and l=10 cm), bare rough (s=3 cm and l=10 cm), and vegetated (LAI=3). In above, s denotes the RMS surface height and l is the correlation length of the surface. Bistatic scattering coefficients from the Kirchhoff's rough surface model are used in Peake's approach to calculate microwave emissions from the rough surface. For vegetated terrain, the canopy parameters from a typical soybean field are chosen for the modeling (Table 3). The leaf dimensions and density of the soybean canopy are equivalent to a canopy of LAI=3. The forward model results at 6 GHz are inverted using the dual polarization technique described earlier. Figure 5 shows the retrieved results for the four types of terrain. The RMS errors in the soil moisture estimation are 14.9, 13.5, 3.2, 0.63 percent for vegetated, bare rough, bare low-roughness and smooth bare terrains, respectively. The estimation has been carried out for the soil moisture range of 0 - 100 percent. (Note that the typical field capacity for agricultural soil is ~ 35 percent).

Table 3. Soybean canopy parameters

Canopy Parameters	
Canopy height	60 cm
Plant density	1000 /m**3
Leaf Parameters	
Radius	4 cm
Thickness	0.2 mm
Density	1000 /m**3
Dielectric Constant	25.3 +j7.96
Inclination Angle	Uniform

* These parameters are derived from actual measurements carried out in a field experiment conducted at the Beltsville, MD USDA facility.

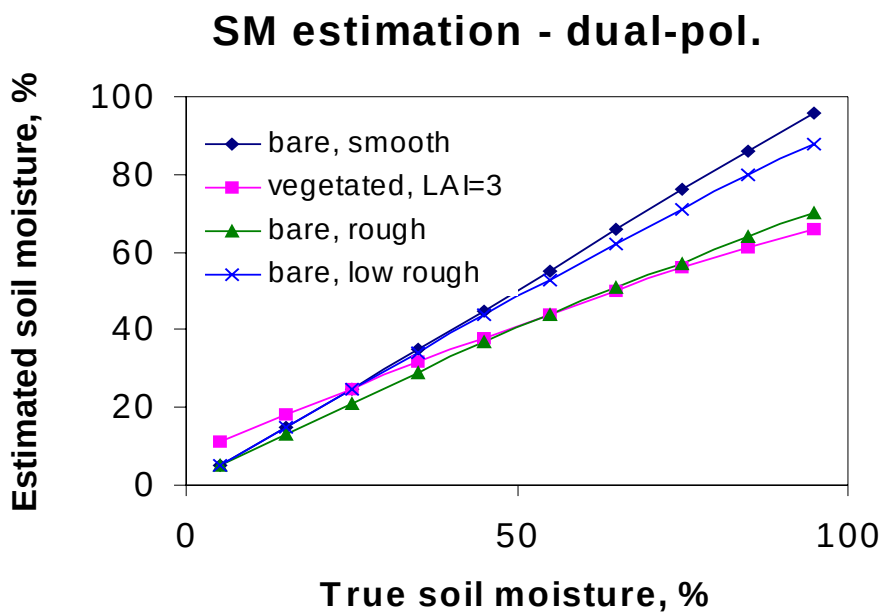

Figure 5. Microwave soil moisture inversion results for four different land surfaces. Dual polarization is used.

3.4.1.2 Error due to Data Accuracy and Precision (E_{m2})

Based on the current Sensor Requirement Document for VIIRS (NPOESS, 1999), the uncertainty and precision requirement in LST are ± 2.5K and ~0.5K, respectively. Similar requirements for CMIS are not known yet. Examining these parameters for SSM/I reveals its accuracy and precision as ± 3K and 0.42K (Hollinger *et al*., 1990). This indicates that the optical/IR and microwave sensors have approximately the same error in accuracy as it does in precision. The uncertainty in LST arises because of the poor knowledge of surface emissivities. (Emissivities are required to convert IR temperature to LST). For SSM/I sensor, the accuracy is poor as a result of calibration problems; however, NEDT (noise equivalent temperature differential) is small ~ 0.42K.

Microwave soil moisture is essentially derived from microwave emissivity, which is proportional to the ratio of microwave brightness temperature to LST (see Equation 3). Because of ratioing, the effect of accuracy and precision in the microwave estimation of soil moisture is very much reduced. To affirm this point, we have chosen a scene (25°N – 35°N, 40°E – 50°E) of February 9, 1991 in Middle East area, near Iraq for the analysis (Chauhan *et al*., 1998). The LST, NDVI and surface albedo are calculated from AVHRR, Level 1B data that has a resolution of ~1 km. A simple split window method (Price, 1984) employing data from Channel 4 and 5 of AVHRR is used for this purpose. Similarly, surface albedo is calculated by scaling data from Channel 4 and 5 of AVHRR. The SSM/I data at 19.4 GHz is at 25 km resolution on cylindrical equal area projection true at 30N and 30S. The microwave algorithm discussed in Section 3.3 is most accurate for the weakly vegetated area. As a result, we have used an upper limit of NDVI $\leq$ 0.4

to limit the vegetated area. All pixels with NDVI>0.4 are discarded in the procedure for microwave estimation of soil moisture. Based on the work of Myneni *et al.* (1997), NDVI of 0.4 translates to LAI ~1 for most biomes except forests where LAI could be ~2 (Figure 5a in Myneni *et al*. [1997]). Because the Middle East area nearby Iraq has very little forested area, we infer that the current scene is lightly vegetated with LAI ~1.

The microwave retrieval algorithm is applied to brightness temperature and LST (aggregated to the microwave i.e., 25 km resolution), and soil moisture is computed. Then both temperatures are corrupted by measurement errors (E) due to precision and/or accuracy. For the calculation of errors for the microwave soil moisture, three cases of measurement error E are considered for the present study; (a) E $=\pm 0.05$K in LST only (from AVHRR) (b) E = ± 1K in microwave brightness temperature only (from SSM/I), and (c) E $=\pm 3$K both in LST and microwave brightness temperature. The SSM/I brightness temperature and/or LST are perturbed randomly around their mean values by $\pm$E. These perturbed temperatures are then used in the microwave estimation algorithm of the soil moisture. The root mean square errors in soil moisture estimates for the above three cases are computed to be 0.063, 0.15 and 0.0045 percent, respectively. These calculations suggest that the accuracy and precision of the two temperatures have relatively small effect on the microwave estimation of the soil moisture.

3.4.2 Error in Soil Moisture Estimation at High Resolution

For soil moisture estimation at high resolution, there are again two different errors; first is the regression error (E_{v1}), and the second is precision error due to NDVI, LST and albedo (E_{v2}). To estimate both of these errors, we have performed further analysis on the Middle East scene of February 9, 1991. A system of linear equations (Equation 9) is set up using SSM/I-derived soil moisture, aggregated NDVI, albedo, and LST for the scene area. The system is solved, and regression coefficients for the second order polynomial fit are determined. The regression coefficients, and optical/IR parameters (NDVI, albedo, and LST) at 1 km are used in the right-hand side of Equation 9 to obtain high-resolution (1 km) soil moisture values for the scene. The regression error is computed as the RMS error between the microwave soil moisture using a regression coefficient and a previous direct estimate of soil moisture from the SSM/I data. For this particular scene, the regression error (E_{v1}) is 1.6 percent. Analysis performed on other scenes also gave the same order of regression error (Chauhan *et al*., 1998). The relatively lower value of regression error indicates that there are enough training data points in regression and the regression coefficients are reasonable.

Table 4. Error budget for the soil moisture estimation algorithm (%)

Error Types	0 –35% (< soil field capacity)	0 –100%	Comment
Microwave Resolution:			
Algorithm Error (E_{m1}):			
Bare smooth	0.0005	0.63	
Vegetated (LAI=3)	3.6	14.9	Objective*
Bare rough	3.7	13.5	Extreme
Bare low rough	0.5	3.2	Typical
Accuracy & Precision error (E_{m2})	< 1	< 1	
High Resolution:			
Regression Error (E_{v1})	1.6	1.6	
Precision Error (E_{v2}):			
LST	0.338	0.338	
NDVI	1.57	1.57	
Albedo	0.722	0.722	

For 0 – 100% soil moisture range

Error budget $= \sqrt{3.2^2 + 1^2 + 1.6^2 + .338^2 + 1.57^2 + .722^2}$

< 5 % for a typical bare rough surface

*For vegetated surface, the microwave algorithm is limited to weak vegetation i.e., NDVI ~ 0.4 or LAI ~1. Therefore, microwave algorithm error E_{m1} would be much lower than 14.9%

To compute E_{v2}, we have flowed down precision error in LST, NDVI, and albedo to the high-resolution soil moisture algorithm. We have assumed precision (P) in LST, albedo, NDVI as 0.5K, 0.020, 0.02, respectively. These precision values are taken directly from the Sensor Requirement Document of VIIRS/NPOESS (NPOESS, 1999). One-by-one, the three inputs are perturbed randomly around their mean value by $\pm$P. The soil moisture resulting from perturbed input to Equation 12 are compared to that obtained from the unperturbed inputs. The root mean square error (E_{v2}) due to precision in LST, NDVI and albedo are computed to be 0.338, 1.57 and 0.722 percent, respectively.

An examination of Equation 12 reveals that the microwave-derived soil moisture M is related to the scene variations in NDVI , albedo and LST and not to their absolute values. The parameters NDVI*, A*, and T* in Equations 8, 9, and 13 define these relative variations. Therefore, accuracy of NDVI, LST and albedo is likely to have little effect on the high-resolution soil moisture estimation. Consequently, we have not calculated the effect of accuracy in LST, NDVI and albedo on the soil moisture estimation procedure.

Assuming that different sources of error are uncorrelated, the total error budget for soil moisture can be calculated as $\sqrt{E_{m1}^2 + E_{m2}^2 + E_{v1}^2 + E_{v2}^2}$. Based on these error budget calculations, the

maximum error to fulfill threshold requirement (typical bare surface) is less than 5 percent. For vegetated surface (an objective requirement), the error is higher. This error is well within the requirements set by NPOESS for the soil moisture estimation (NPOESS, 1999). Note that all but the microwave algorithm errors are computed for the satellite data of Feb. 9, 1991 for the Middle East scene. A summary of all the errors is given in Table 4.

3.4.3 Calibration Errors

VIIRS soil moisture EDR is not estimated directly from VIIRS sensor response. Rather it is estimated from VIIRS products/radiances and CMIS brightness temperature. Currently, we are insulated from CMIS system design activities, so CMIS instrument errors are not known to us. The calibration error effects on NDVI, LST, and surface albedo are discussed in their respective ATBDs.

3.4.4 Instrument Noise

The effects of VIIRS instrument noise on NDVI, LST, and surface albedo are discussed in their respective ATBDs.

3.4.5 Others

The regression error can increase if the training area (where regression coefficients are derived) and the test area (where regression is applied) are not the same. One such case can be the area where the swath widths of VIIRS and CMIS do not overlap. Current SRD defines VIIRS and CMIS swath-widths as 1,700 km and 3,000 km respectively. Later versions of this ATBD will provide estimates of this error.

3.5 PRACTICAL CONSIDERATIONS

3.5.1 Numerical Computation Considerations

At this stage of the ATBD development process, we are adopting a modularization approach so that the modules from one EDR can be shared with others. The algorithms are combined in a pipeline so as to facilitate all the VIIRS EDR simulation processes. Existing computations for soil moisture EDR are very fast, and computation time is not an issue for this EDR.

3.5.2 Programming and Procedural Considerations

All programming is in FORTRAN, and the images are produced using ERDAS image processing software.

3.5.3 Configuration of Retrievals

In development.

3.5.4 Quality Assessment and Diagnostics

Soil moisture quality flags are being developed. The EDR values will be flagged if, for some reason, the requirements given in *[V-2]* are not met. A typical example might be the case of soil

moisture EDR beyond the swath width of 1700 km. Because the LST could be of lower quality in swath widths greater than 1700 km, it could affect the soil moisture estimate. Soil moisture estimates from difficult terrain such as mountains may also be flagged.

3.5.5 Exception Handling

At this stage of the ATBD development process, this issue is under consideration.

3.6 ALGORITHM VALIDATION AND DISCUSSION

There is a dearth of large scale soil moisture *in situ* data for the validation of retrieval results. In addition, all *in situ* measurements are point measurements, and there are unresolved issues concerning comparing point measurements with soil moisture maps. We have followed an approach in which different components of the algorithm are tested/validated separately by using a combination of simulated data from a well tested forward model as well as from satellite data. The error budget discussed earlier revealed different types of errors. In this section, the algorithm is applied to a mid-west region of the United States and the soil moisture estimates are compared with *in situ* data. Parameters such as horizontal cell size, horizontal reporting interval, mapping uncertainty, and minimum swath width are not discussed here as their verifications are the same as those for NDVI or LST or albedo. Among the remaining parameters Vertical Cell Size is not fixed for all soil types and for all soil moisture levels and Cell size verification is not relevant. The soil moisture estimates are from the skin layer of the soil surface.,

3.6.1 Application to SGP-97 Data

Validation of soil moisture estimation results is difficult and even more so if satellite data is involved. The difficulty lies not only in the estimation process but also in the measurements of soil moisture. Several issues are involved in soil moisture measurements. Microwave sensors measure soil moisture in the topmost soil layer (1/10 to 1/4 of a wavelength). At 19 GHz, this layer can be about 0.1-0.4 cm deep. The penetration of the microwave signal depends on soil moisture itself. In view of this, it is difficult to decide the depth of soil samples for *in situ* measurements. Soil moisture changes very rapidly in the top layer. In addition, there are practical problems in collecting soil samples at this depth. Also, spatial distribution of soil moisture depends on soil parameters which are not distributed homogeneously in the area. As a result, average soil moisture computed from point measurements in a footprint area may not be a correct representation of the soil moisture in the footprint. In view of these uncertainities, a close comparison of *in situ* point measurements from SGP-97 with the soil moisture predictions is not attempted here. Rather the temporal and spatial comparisons with data are made here.

The algorithm is applied to data over a mid-west region (33°N to 38°N, -100°W to -96°W) covering the SGP experiment conducted in June-July of 1997. The experiment was designed to measure and estimate spatial and temporal variation in soil moisture and other hydrologic variables. The bulk of this region is grassland along with short vegetation in the agricultural fields. A major component of the experiment was to conduct a large number of point measurements of 0-5 cm deep gravimetric soil moisture. These measurements were made at three locations i.e., Little Washita (LW), El Reno (ER), and Central Facility (CF). The relative locations of these sites are shown in Figure 6.

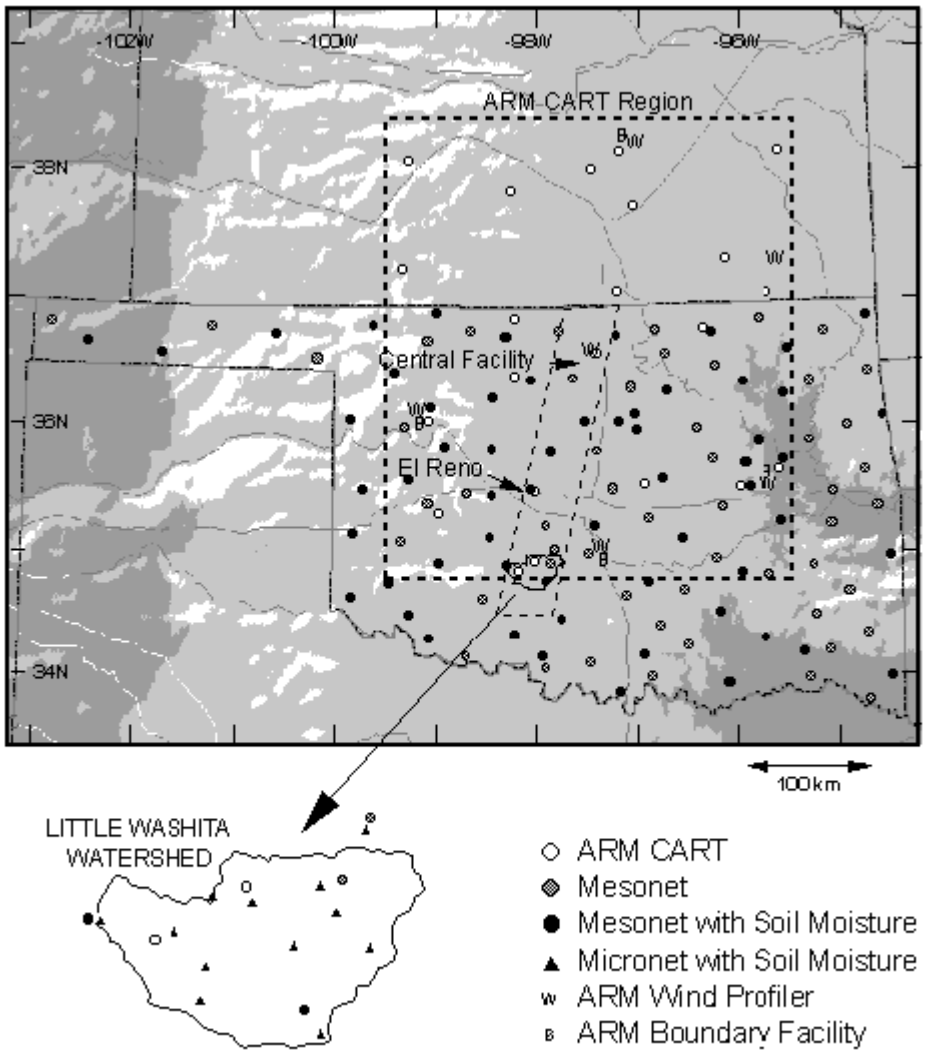

Figure 6. Location of three sites for the *in situ* soil moisture measurements at the SGP-97 experiment.

At each of the locations, several fields were selected and within a field, several measurements of soil moisture were made almost daily for about a month. Efforts were made to collect daily soil moisture samples in the same general vicinity to facilitate temporal comparisons of soil moisture. A specific pattern to walk in and out of the fields was followed More details of the experiment and data can be found at http://hydrolab.arsusda.gov/SGP-97.

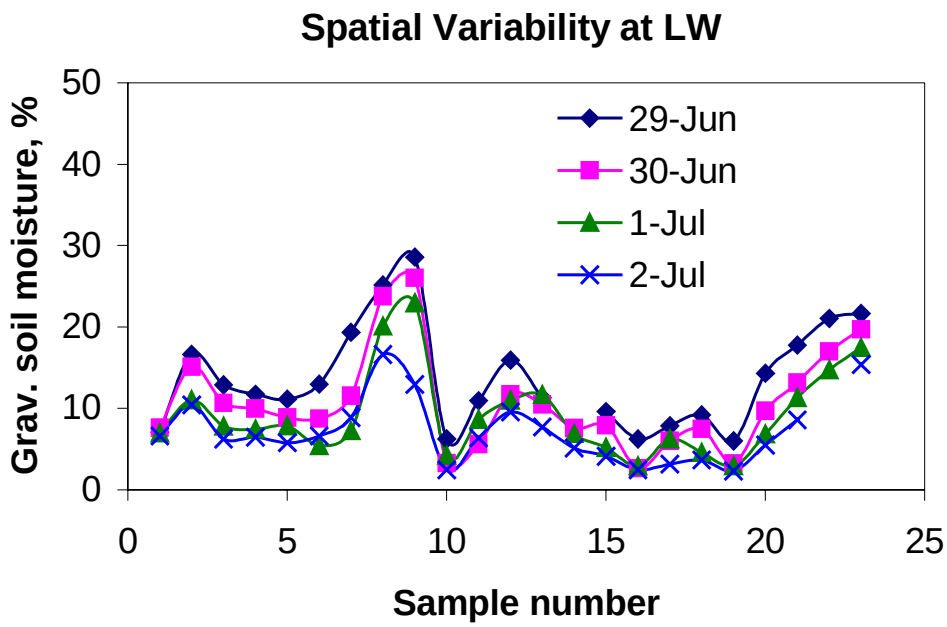

Figure 7. An example of spatial variability in 0-5 cm soil moisture in a particular field at Little Washita. The variability appears to be consistent for all the four days considered in the present study.

For the present analysis, four days (June 29-30, July 1-2) during the SGP-97 experiment with relatively clear sky conditions, were selected. Figure 7 shows the measured soil moisture variability at LW on the four days. It is noticed that there is a definite pattern in spatial variability of soil moisture that repeats itself on all the four days. This variability could be the result of changing soil properties of the area. Similar variability is also noticed in the soil moisture data from other locations at ER and CF. The plots showing spatial variability at ER and CF are not given here.

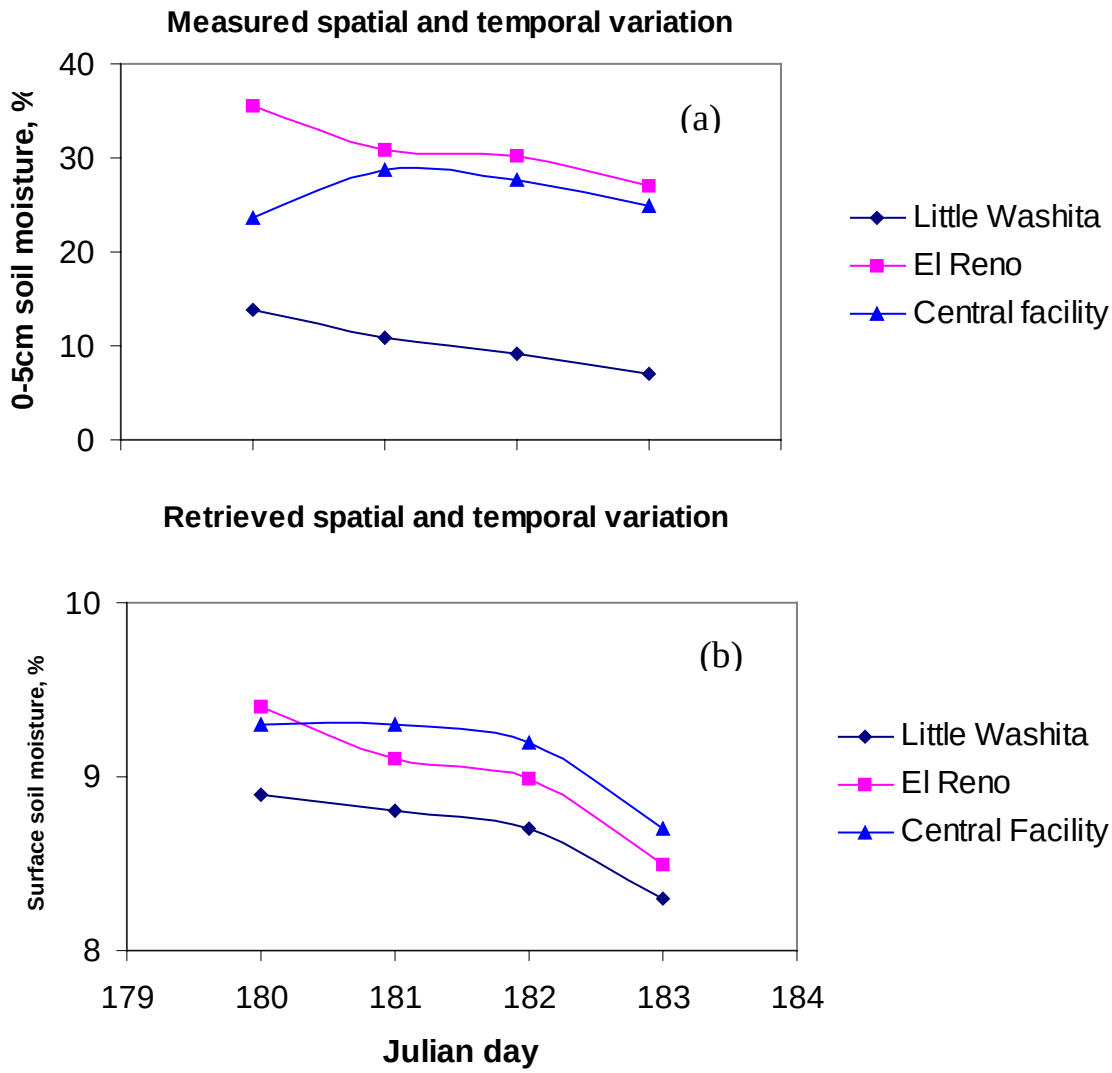

Figure 8. (a) An example of temporal and spatial variability in 0-5 cm soil moisture measured at the SGP-97 area. Point measurements from each location such as LW are averaged from the data collected from many fields in LW. LW and CF are located at south and north edge of the SGP-97 experimental area. (b) Retrieved surface soil moisture averaged over three locations for June 29-30, July 1-2, 1999. The averaging is done in a 5km x 5km area for a particular location. Note that pixels averaged in (a) and (b) are not identical.

To determine if there is a temporal and spatial pattern/trend in soil moisture at these three locations, the soil moisture measurements from all samples for a particular location on a given day are averaged and the results are plotted in Figure 8a. Note that the averaging of soil moisture at a particular location is based on point measurements and the previous figure i.e., Figure 7, shows a typical variability in those measurements. Except for CF on June 29, soil moisture decreases from June 29 to July 2. Notice also that soil moisture in the northern location

(i.e., CF and ER) is higher than soil moisture in the southern location i.e., at LW.

In addition to soil moisture *in situ* data, satellite data from AVHRR and SSM/I (frequency=19.4 GHz) were also acquired for the four days over the SGP-97 experiment region. This data has been analyzed (similar to the Middle East scene) for the estimation of soil moisture. The dual polarization method is employed and the microwave algorithm is limited to weakly vegetated pixels. All pixels with *NDVI*>0.4 are discarded for estimating soil moisture and the derivation of the regression relations. To estimate soil moisture at 1 km resolution, a system of linear equations are set up using SSM/I-derived soil moisture, aggregated *NDVI*, albedo, and *LST*. The system is solved and the regression coefficients for the SGP-97 region are determined. The RMS error between the regression-derived soil moisture and the SSM/I-derived soil moisture is small (~ 0.01 for all days). The soil moisture values at 1 km are obtained by substituting 1 km scale *NDVI*, albedo, and LST on the right-hand side of (9). Soil moisture estimates are averaged over a 5 km x 5 km area for each of the LW, ER and CF locations. The 5 km x 5 km area could contain roads and buildings and may not fully represent the sampled areas. Figure 8b shows a plot of volumetric, high-resolution soil moisture predictions for the four days at the three sites. A comparison of Figures 8(a) and 8(b) shows that the temporal trend in the predicted soil moisture agrees with the generally decreasing soil moisture trend in the measurements. Also, the lower soil moisture value at the southernmost location (LW) is in agreement with the measurements. The predicted soil moisture is for skin layer only and therefore, comparison of its magnitude with *in situ* measurements is not warranted.

Comparison is also made between the low- and high-resolution soil moisture estimates for the whole SGP-97 region. Volumetric soil moisture from all the pixels in the scene is plotted for the four days. The high resolution soil moisture plot is shown in Figure 9. The soil moisture from the SGP-97 experiment region exhibits a dry-to-moderate level of surface soil moisture. The volumetric soil moisture results at 25 km resolution are plotted in Figure 10. A comparison of Figures 9 and 10 reveals one-to-one relationships between microwave-derived soil moisture and 1 km soil moisture. The two sets of plots also show that the mean value of soil moisture in the two cases is about the same.

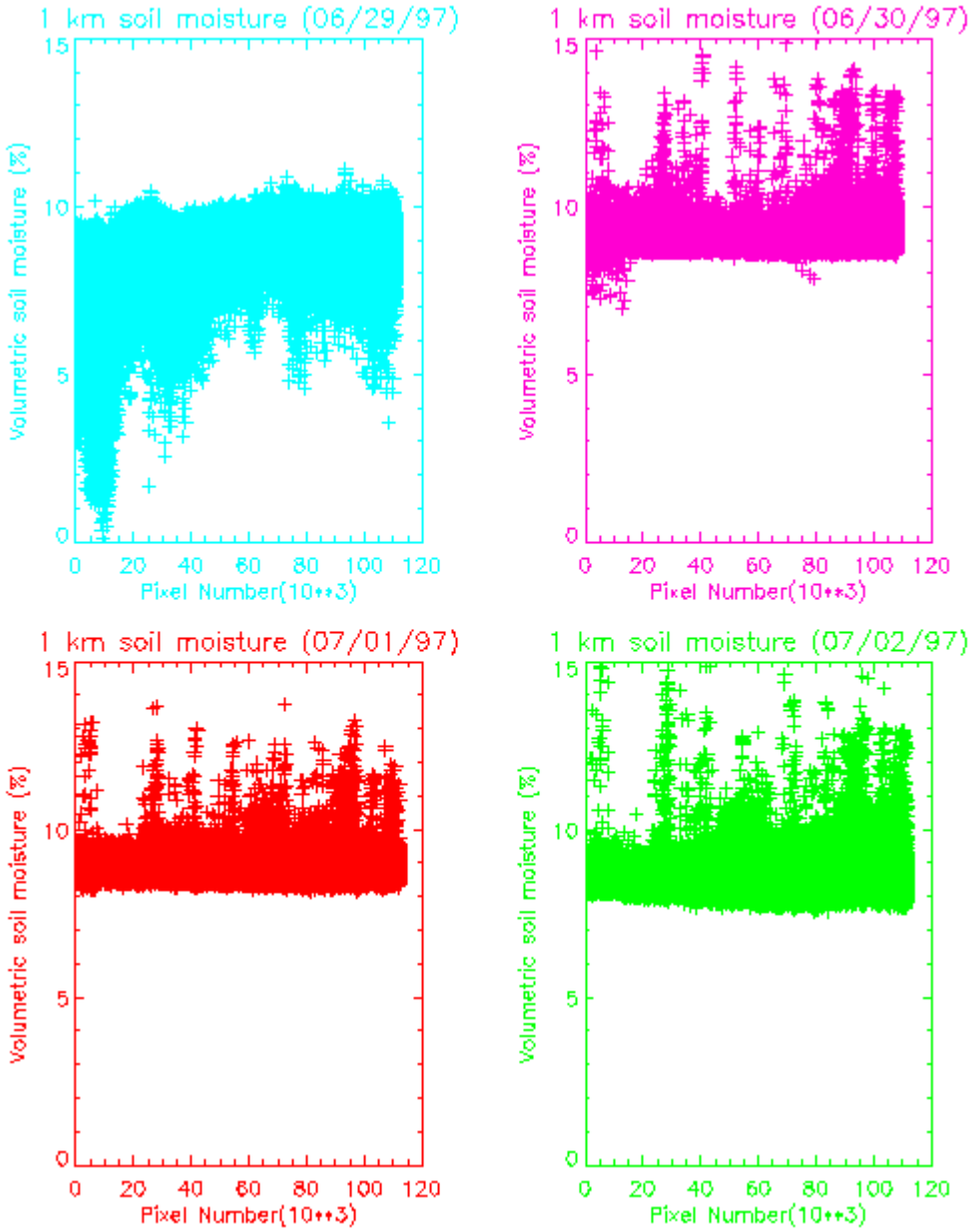

Figure 9. High resolution soil moisture plot for the SGP-97 region for 4 days. Soil moisture range varies from 5-20 percent.

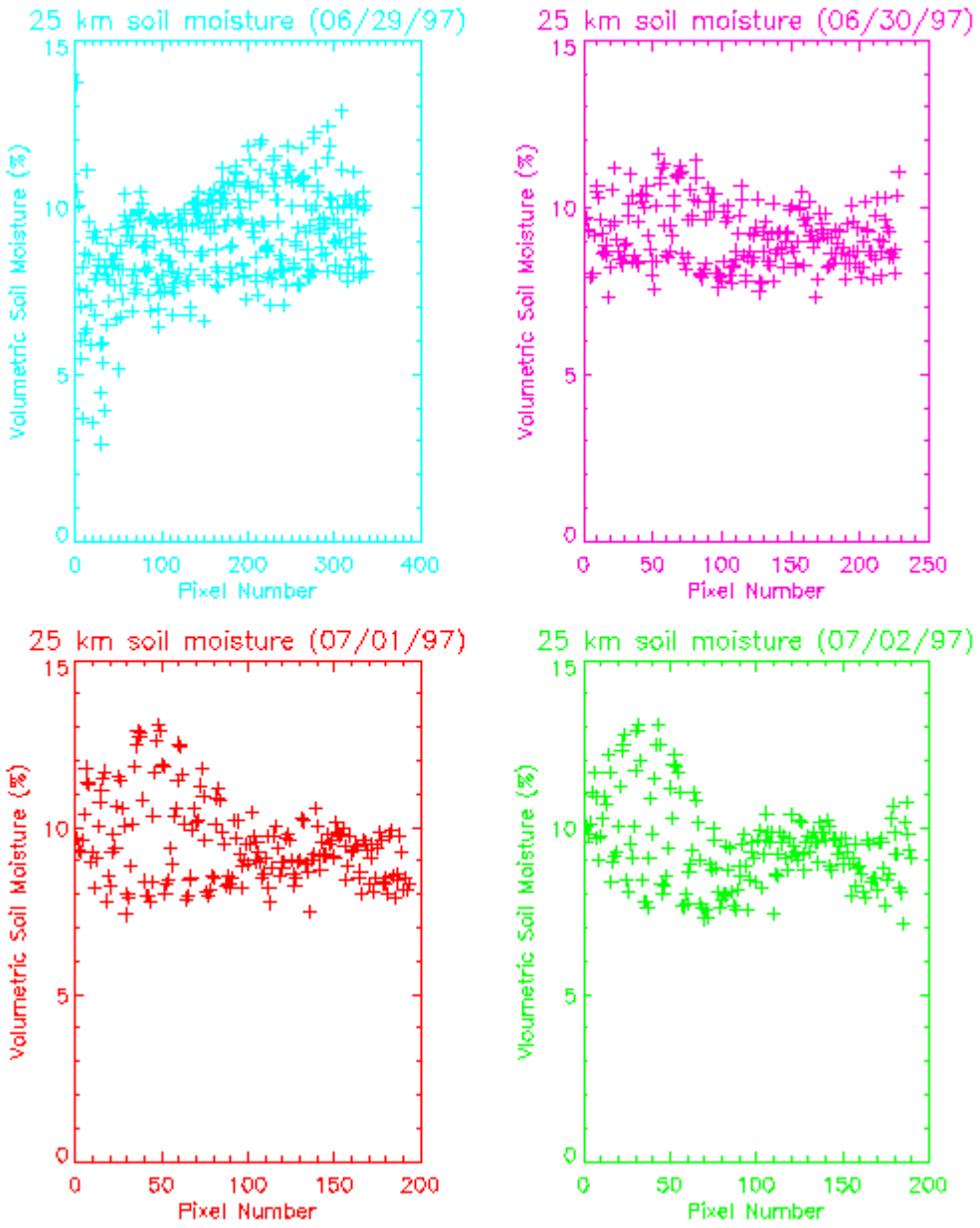

Figure 10. A plot of microwave (low-resolution) of soil moisture for the SGP-97 area. One-to-one correspondence between Figs. 9 and 10 is observed.

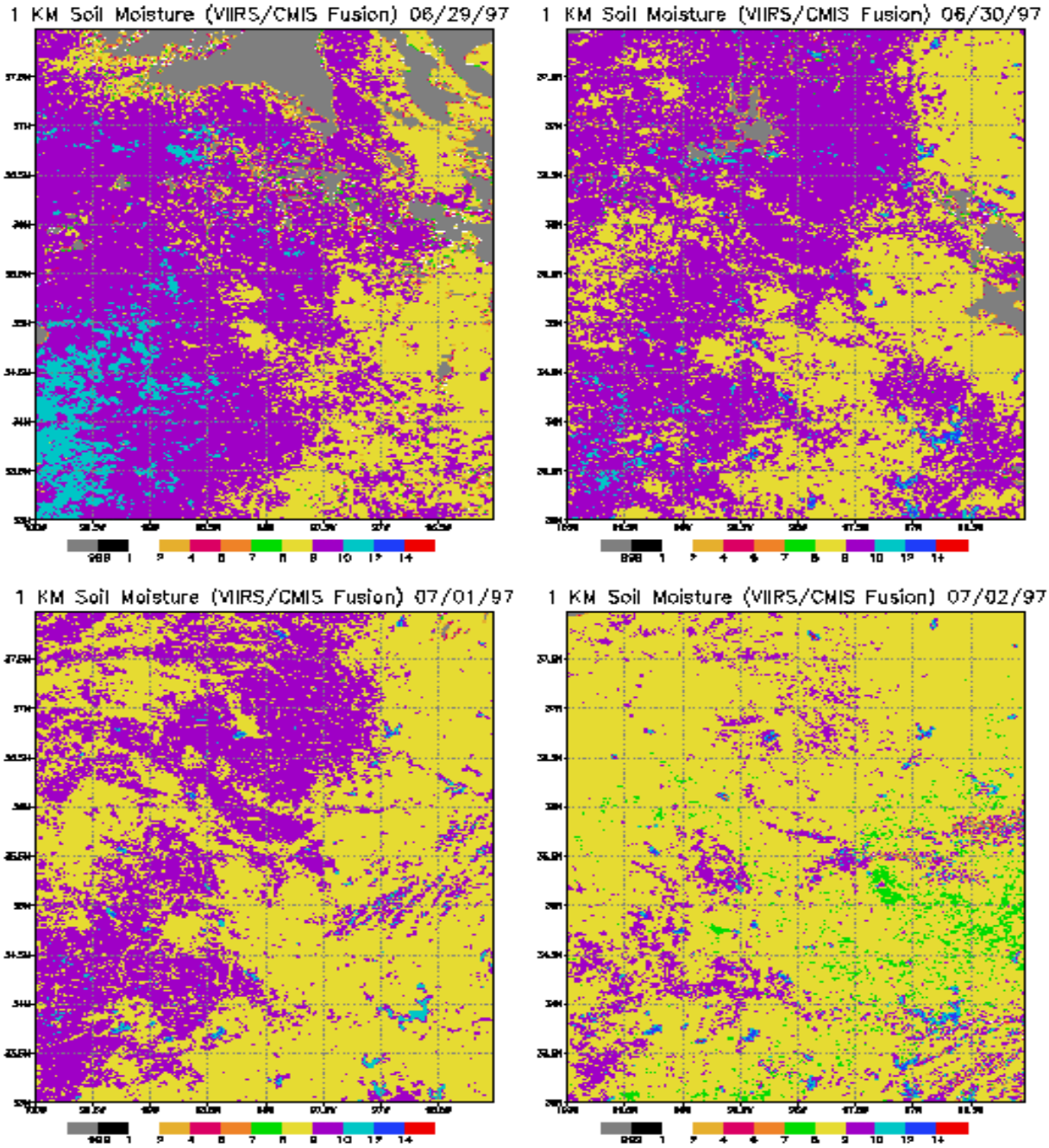

Figure 11. Soil moisture map of the SGP-97 area at 1 km resolution. Decreasing trend in soil moisture from June 29 to July 2 is broadly consistent with data.

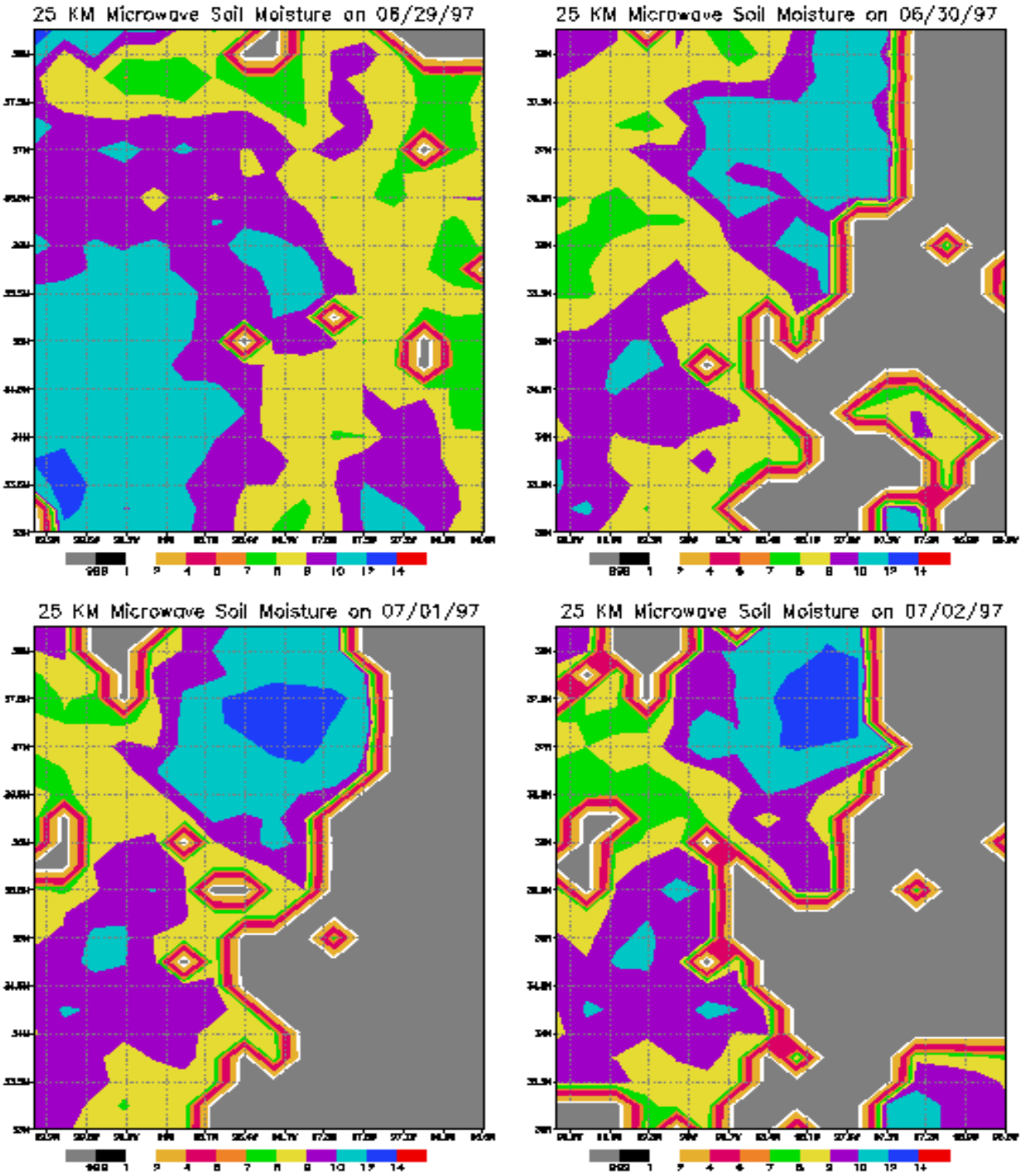

Figure 12. Soil moisture map of the SGP-97 area at 25 km resolution.

To display the results presented in Figures 9 and 10 in terms of soil moisture image maps, the soil moisture values at the low- and high-resolutions are color-coded and mapped to the SGP-97 area grid. The soil moisture images at the two resolution scales are shown in Figures 11 and 12. The aim is to compare the spatial patterns in the soil moisture in the low- and high-resolution images. A visual inspection of the two images shows that there is a close resemblance between the soil moisture spatial patterns and the quantitative estimates. Clearly, the 1 km soil moisture image shows much more detail than the 25 km soil moisture image. The patches of no data in the northern part on June 29 are the result of the cloud mask that was applied to *NDVI*, *LST*, and albedo. Clouds also effect brightness temperature, but the effect is less severe. We have used a simple-minded cloud mask that involves masking cloud pixels based on the visible channel of AVHRR. A new cloud mask for the NPOESS is being developed and will be incorporated in later studies. The eastern part of the SSM/I-derived soil moisture image on June 30, July 1-2 is also shaded gray because SSM/I data was unavailable.

3.6.2. Discussion

The core of the process for high-resolution soil moisture determination involves a synergistic analysis of microwave-optical/IR data. The algorithm combines the traditional accuracy of microwave sensors for soil moisture sensing with the high-resolution capability of optical/IR sensors to determine soil moisture estimates at high-resolution. An important component of the retrieval process is the use of dual-polarization microwave data for obtaining surface reflectivity which is later converted to soil moisture. The dual-polarization technique used here is a departure from single polarization techniques that have been used for most of the previous soil moisture estimation work. The dual polarization is suitable for global soil moisture estimation from satellite data because it does not require *a priori* information about vegetation and surface roughness condition. The NDVI is used to limit the application of the dual polarization algorithm to the weakly vegetated pixels.

Vegetation has been assumed as an absorbing medium only and the scattering from vegetation is ignored. Incoherent scattering from the rough surfaces is also not accounted for in the inversion process. Most of the earlier studies involving soil moisture estimation from large-scale experiments such as MACHYDRO-90, Washita-92, Washita-94, SGP-97, have made the same assumption and found reasonable agreement with *in situ* soil moisture data. The proposed dual polarization method for the microwave soil moisture is expected to be an improvement over the previous techniques because incoherent scattering effects are minimized in the ratioing process.

We have performed a sensitivity analysis on the order of polynomial that is used in the regression. Equation 9 represents a second-order polynomial fit between the microwave-derived soil moisture, NDVI, LST, and albedo. The second-order polynomial has seventeen terms in it. We also experimented with higher-order polynomials. A higher-order polynomial is more accurate but less flexible to interpolate soil moisture values outside the range for which the regression coefficients are derived. On the other hand, a low-order polynomial may not be as accurate, but it can interpolate soil moisture values over a wider soil moisture range.

The signals from SSM/I and AVHRR do not sense soil moisture to the same vertical depth. As a result, their soil moisture estimates can differ. Microwave instruments measure soil moisture in the topmost soil layer, and at 19 GHz, this layer can be less than half a centimeter deep. Strictly speaking, the “universal triangle” method relates soil moisture availability (ratio of soil water

content to field capacity) to radiant temperature and fractional vegetation cover (~$NDVI^{*2}$). It is possible that the estimates of soil moisture using the above two methods are different. But in the approach outlined here, the 'universal triangle' method concept is used to establish relations between soil moisture, temperature, albedo, and NDVI. As a result, the regression coefficients could be different if the microwave-derived soil moisture or soil moisture availability is used in Equation 9. However, this will not effect the process of disaggregation that has been employed to enhance spatial resolution of the soil moisture.

The regression error varies from scene to scene and could depend on the size of the scene. In addition, if the training area (where regression coefficients are derived) and the test area (where regression is applied) are the same, the regression error is small. For the NPOESS soil moisture, we propose to determine separate regression coefficients for each contiguous scene in the orbit. This will ensure reduced regression error. In cases, where the swath widths of VIIRS and CMIS do not overlap, the regression coefficients from the adjacent scene will be used and as a result, the error in soil moisture estimation will be higher.

The technique described here to link low-resolution soil moisture with the land parameters has its theoretical basis in the surface energy balance technique. The "universal triangle" is the result of numerous simulations carried out using the soil vegetation atmosphere transfer modeling. The simulations have also been validated using data from different field experiments (Gillies *et al*. 1997). The SVAT simulations require micrometeorological and other data. Early simulations were conducted using data collected at a field campaign in Mahantango, during the MACHYDRO-90 experiment. In the remote sensing applications a regression relation like Equation 8 gives results similar to those obtained by the SVAT model (http://www.essc.psu.edu/~tnc). Sensitivity tests have shown that the distribution of isopleths inside the triangle is very insensitive to the initial conditions and so one can use a single polynomial to represent a wide range of surface climate conditions and land surface types (Carlson, 1998).

3.6.3 Risks and Risk Reduction Efforts

So far we have identified the four main risk areas. These areas and their potential effect are identified below, along with our plans to mitigate the risks.

1. *Soil moisture from vegetated areas*. Soil moisture from vegetated areas is a research issue and its estimation can affect measurement uncertainty. Soil moisture estimation uncertainty will increase with increasing vegetation cover. As a mitigation plan, we will limit vegetation up to an NDVI<0.4 in the microwave estimation algorithm.

2. *Soil moisture from very rough surfaces.* This also can result in an increase of measurement uncertainty. There are three mitigation plans:

   a) Use dual polarized rather than a single polarization technique for CMIS data inversion.

   b) Determine whether a single roughness parameter (such as the h-parameter from Choudhury, 1993) can be established from simulations that can be used for most of the surfaces for a given viewing geometry (if single polarization method is to be used).

   c) Search for a new technique involving a polarization index that can be applied on any type

of surface roughness and that could be more robust for soil moisture retrievals from heavily vegetated areas.

3) *Soil moisture range.* No work has been performed on soil moisture estimation beyond the field capacity, and very little information exists on soil moisture beyond the field capacity. As a result, we may not be able to validate soil moisture in the full range (0-100 cm/m). Microwave does sense soil moisture in its full range 0-100 cm/m, but whether the regression model is able to translate high-end (beyond field capacity) soil moisture at 1 km resolution will have to be validated against *in situ* data. We plan to participate in some NASA/USDA experiments to validate this issue.

4) *Combining VIIRS and CMIS Synergistic data.* Soil moisture estimates can be different from the two sensors. CMIS and VIIRS do not sense soil moisture in the same vertical cell size. As a result, their soil moisture estimates can differ. We will seek clarification from the Integrated Program Office as to how it plans to benchmark soil moisture.

4.0 ASSUMPTIONS AND LIMITATIONS

4.1 ASSUMPTIONS

In the VIIRS soil moisture retrieval algorithm, we assumed that the dependence of soil moisture on parameters other than NDVI, LST, and surface albedo was weak and was ignored in the regression analysis.

In calculating regression coefficients for a particular scene, we assumed that the scene area was large enough to provide sufficient data points for regression, but too small to cause any significant change in solar radiation flux across the scene.

It is assumed that the widely accepted empirical relationship between the dielectric constant and volumetric soil moisture is valid up to 100 percent soil moisture. Based on current soil physics, however, water added to soil beyond its field capacity is not retained by the soil. Field capacity varies by soil type: from 4 percent (by mass) in sand, to 45 percent in heavy clay soils, and up to 100 percent in certain organic soils.

For the cloudy worst case, there is no way to derive soil moisture from VIIRS, which operates in the visible/infrared bands. Therefore, the only source for soil moisture information is from microwaves (i.e., CMIS). Based on the resolution of CMIS, 20 km or more can be the highest achievable resolution. The soil moisture EDR for cloudy conditions under VIIRS has the same requirements as that under CMIS. Therefore, for cloudy conditions, the VIIRS soil moisture EDR will be same as the CMIS soil moisture EDR. Currently, we are not duplicating the CMIS effort, but we have the capability to do so, and we will produce soil moisture under cloudy conditions if needed.

4.2 LIMITATIONS

The algorithm is limited to bare soils and weakly vegetated areas. Its application to moderate and heavily vegetated areas could yield inaccurate results.

The accuracy of VIIRS soil moisture algorithm will be degraded beyond a swath-width range of 1,700 km.

Microwave instruments measure soil moisture in the topmost soil layer ($1/10^{th}$ to $1/4^{th}$ of a wavelength). The optical/IR sensors may not be sensitive at the same depth. It is possible that the microwave estimates of soil moisture may not be as strongly related to NDVI, LST and albedo as its optical/IR equivalent.

Soil moisture is a defined quantity for land only. Land covered with snow, ice, or water will be reported as 100 percent since the soil moisture will be reported for the skin layer. No soil moisture will be reported for the frozen soils and forested areas. Soil moisture from difficult terrain such as mountains will be flagged. Mountains usually have rocks, stones, and trees on their surfaces. In addition, their large slopes affect the local viewing angle geometry. As a result, soil moisture estimations are of questionable value and may not always satisfy accuracy requirements given in the VIIRS SRD. Very little exists in the literature about soil moisture from mountains.

Remote sensing measurements of soil moisture beyond the field capacity of soil (i.e., when the soil becomes saturated and cannot drain water) may not be reliable. Furthermore, remote sensing measurements of soil moisture beyond the field capacity are not generally available in open literature. Measurement range accuracy is limited in the range from 0 to soil field capacity. For most soil surfaces, the field capacity is ~0.4. None of the existing techniques have been tested for soil moisture range beyond the field capacity.

The soil moisture uncertainty range is limited to bare soils and low-vegetated areas. Large vegetation, such as forest and orchards, are included.

The soil moisture EDR swath width is limited by the swath width of the LST EDR (1700 km). Less accurate soil moisture will be produced beyond the 1,700 km swath because the LST beyond the 1,700 km swath could be less accurate.

5.0 REFERENCES

Basharimov, A., and A. Shutko (1975). Simulation studies of SHF radiation characteristics of soils under moist conditions. NASA Technical Translation TT-F-16, 489, NASA, Washington, DC.

Beljaars, A., P. Viterbo, M. Miller and A. Betts (1996). The anomalous rainfall over the United States during July 1993: Sensitivity to land surface parameterization and soil moisture anomalies. *Mon. Weath. Rev.*, vol. 124, pp. 362-383.

Brubaker, L., and D. Entekhabi (1996). Analysis of feedback mechanisms in land-atmosphere interaction. *Water Resour. Res.*, vol. 32, pp. 1343-1357.

Carlson, T., R. Gillies, and E. Perry (1994). A method to make use of thermal infrared temperature and NDVI measurements to infer surface soil water content and fractional vegetation cover. *Remote Sensing Reviews*, vol. 9, pp. 161-173.

Carlson, T. (1998). Personal Communication.

Chauhan, N. (1999a). Soil moisture estimation: An operational approach. *IEEE Transactions on Geosci. and Remote Sens*., submitted.

Chauhan, N., D. LeVine and R. Lang (1999b). Passive and active remote sensing of soil moisture under a forest canopy. *IEEE Transactions on Geosci. and Remote Sens*., submitted.

Chauhan, N., L. Di, S. Miller and P. Ardanuy (1998). Soil moisture visible/infrared imager/ radiometer suite algorithm theoretical basis document - Version I. SRBS Document # Y2387, Raytheon, Lanham MD 20706.

Chauhan, N. (1997). Soil moisture estimation under a vegetation cover: combined active passive remote sensing approach. *Int. J. Remote Sens*., vol. 18, pp. 1079-1097.

Chauhan, N., D. LeVine, and R. Lang (1994). Discrete scatter model for radar and radiometer response to corn: comparison of theory and data. *IEEE Trans. Geosc. & Remote Sens.*, vol. 32, pp. 416-426,1994.

Choudhury, B. (1993). Reflectivities of selected land surface types at 19 and 37 GHz from SSM/I observations. *Remote Sens. Environ.*, vol. 46, pp. 1-17.

Cracknell, A., and Y. Xue (1996). Thermal inertia determination from space – a tutorial review. *Int. J. Remote Sens.*, vol. 17, pp. 431-461.

Delworth, T., and S. Manabe (1989). The influence of soil wetness on near surface atmospheric variability. *J. Clim.*, vol. 2, pp. 1447-1462.

England, A., J. Galantowicz, and M. Schretter (1992). The radiobrightness thermal inertia measure of soil moisture. *IEEE Trans. Geosci. and Remote Sens.*, vol. 30, pp. 132-139.

Engman, T. (1991). Application of remote sensing of soil moisture for water resources and agriculture. *Remote Sensing of Environ.*, vol. 35, pp. 213-226.

Gillies, R., T. Carlson, W. Kustas, and K. Humes (1997). A verification of the "triangle" method for obtaining surface soil water content and energy fluxes from remote measurements of the Normalized Difference Vegetation Index (NDVI) and surface radiant temperature. *Int. J. Remote Sens.*, vol. 18, pp. 3145-3166.

Hallikainen, M., F. Ulaby, M. Dobson, and M. El-Rayes (1985). Dielectric behavior of wet soil-Part I: Empirical models and experimental observations. *IEEE Transactions on Geosci. and Remote Sens*., vol. 23, pp. 25-34.

Hollinger J. J. Pierce and G. Poe (1990). SSM/I instrument evaluation. *IEEE Transactions on Geosci. and Remote Sens*., vol. 28, pp. 781- 790.

Idso B., T. Schmugge, R. Jackson, and R. Reginto (1975). The utility of surface temperature measurements for remote sensing of soil water studies. *J. Geophys. Res*., vol. 80, 3044-3049.

Idso, S., R. Jackson, and R. Reginato (1976). Compensating for environmental variability in the thermal inertia approach to remote sensing of soil moisture. *J. of Applied Meteor*., vol. 15, pp. 811-817.

Jackson, T., and D. LeVine (1996). Mapping surface soil moisture using an aircraft-based passive instrument: algorithm and example. *J. of Hydrology*, vol. 184, pp. 85-99.

Jackson, T., T. Schmugge, and J. Wang (1982). Passive sensing of soil moisture under vegetation canopies. *Water Resources Research*, vol. 18, pp. 1137-1142.

Jackson, T. (1997). Soil Moisture estimation using special satellite microwave/imager satellite data over a grassland region. *Water Res.*, vol. 33, pp. 1475-1484.

Lang, R. and J. Sidhu (1983). Electromagnetic backscattering from a layer of vegetation: A discrete scatter approach. *IEEE Transactions on Geosci. and Remote Sens*., vol. 21, pp. 62-71.

Myneni, R., R. Nemani, and S. Running (1997). Estimation of global leaf area index and absorbed PAR using radiative transfer models. *IEEE Trans. Geosc. & Remote Sens.*, vol. 35, pp. 1380-1393.

Nemani, R., S. Running, L. Pierce, and S. Goward (1993). Developing satellite derived estimates of surface moisture status. *Journal of Applied Meteorology*, vol. 32, pp. 548-557.

Njoku, E. and L. Li (1999). Retrieval of land surface parameters using passive microwave measurements at 6-18 GHz. *IEEE Transactions on Geosci. and Remote Sens*., vol. 37, pp. 79-93.

NPOESS, (1999). Sensor requirements for the VIIRS/NPOESS sensors, Integrated program Office, Silver Spring, MD 20910.

O'Neill, P., N. Chauhan, T., and Jackson (1996). Use of active and passive remote sensing for soil moisture estimation through corn. *Int. J. Remote Sens.*, vol. 17, pp. 1851-1865.

Owe, M., Van de Griend and A. Chang (1992). Surface moisture and satellite microwave observations in semi-arid Southern Africa. *Water Res.*, vol. 28, pp. 829-839.

Peake, W. (1959). Interaction of electromagnetic waves with some natural surfaces. *IRE Trans. Antennas Propag.*, vol. AP-7, pp. S324-S329.

Price, J. (1977). Thermal inertia mapping: A new view of the Earth. *J. Geophy. Res.*, vol. 82, pp. 2582-2590.

Price, J. (1984). Land surface temperature measurements from the split window channels of the NOAA-7/AVHRR. *J. Geophy. Res.*, vol. 89, pp. 7231-7237.

Saatchi, S., D. LeVine and R. Lang (1994). Microwave backscattering and emission model for grass canopies. *IEEE Transactions on Geosci. and Remote Sens*., vol. 32, pp. 177-186.

Seller, P., Y. Mintz, Y. Sud and A. Dalcher (1986). A simple Biosphere model (SIB) for use within general circulation models. *J. Geophy. Res.*, vol. 43, pp. 505-531.

Tsang, L, J. Kong, and R. Shin (1985). Theory of Remote Sensing. (New York: John Wiley & Sons).

Ulaby, F., M. Moore, and A. Fung (1982). Microwave remote sensing: Active and passive, vol. I-III. Reading, MA: Addison-Wesley Publishing Co.

Van de Griend, A., and M. Owe (1993). Determination of vegetation optical depth and single scattering albedo from large scale soil moisture and Nimbus/SMMR satellite observations. *Int. J. Remote Sens.*, vol. 14, pp. 1875-1886.

APPENDIX

MICROWAVE EMISSION MODEL FOR LAND

Microwave radiometer response is obtained by summing up all the energy over the hemisphere above the forest canopy. We have followed Peake's approach (1959) which assumes thermal equilibrium so that energy absorbed is equal to the energy emitted. The emitted energy or emissivity is expressed as one minus the scattering albedo (Ulaby *et al*., 1982), and therefore, the microwave brightness temperature T_q ($q \in h, v$) can be computed as

$$T_q = (1 - W_q)T \tag{A1}$$

where T is the physical temperature of the scene, W_q is the scattering albedo and is made up of specular and diffused components i.e., $W_q = W_q^{diff} + W_q^{spec}$, where W_q^{diff} and W_q^{spec} are diffused and specular albedos respectively. These albedos are scene albedos and are different from the single scattering albedo. A schematc representation of the model is given in Figure A1.

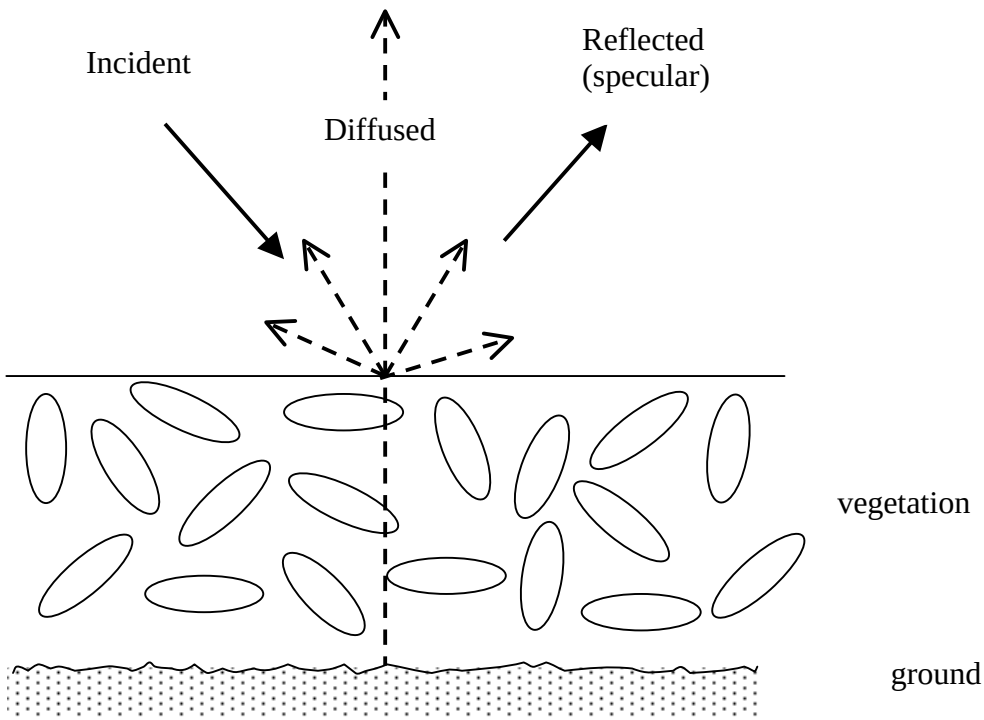

Figure A1. Schematic representation of the emission model for vegetated terrain based on Peake's approach.

The specular albedo for a vegetated rough surface is given as

$$W_q^{spec} = \Gamma_{sq}\Gamma_{iq}^{*}\ e^{-2\tau_q} e^{-4k_o^2 s^2 \cos^2\theta_i} \tag{A2}$$

where Γ_{iq} and Γ_{sq} are the Fresnel reflection coefficients of the flat surface in the incident and the scattered (specular) direction respectively. The asterisk (*) over Γ_{iq} denotes its complex conjugate. Earlier in Section 3.3 we used R_g^h and R_g^v to denote the reflection coefficients which are a real part of Γ_{iq}. The diffused albedo from a vegetated rough surface is contributed both by the vegetation and the rough surface. It can be expressed as sum of the vegetation and rough surface albedos. Mathematically, either one of the latter can be obtained by integrating the scattering coefficients over the hemisphere above the scene as (Chauhan *et al*., 1994)

$$W_q^{diff} = \frac{1}{4\pi\cos\theta_i}\int\left[\sigma_{hq}^{o}(\mathbf{o},\mathbf{i}) + \sigma_{vq}^{o}(\mathbf{o},\mathbf{i})\right] d\Omega_s \tag{A3}$$

where $\sigma^o(\mathbf{o},\mathbf{i})$ are bistatic scattering coefficients of the vegetation or the rough surface. These are calculated using distorted Born approximation (Lang and Sidhu, 1983) and Kirchhoff's rough surface approach (Ulaby *et al*., 1982) for the vegetation and rough surface, respectively. The integration is carried over the upper hemisphere where $d\Omega_s = \sin\theta_s\, d\theta_s d\varphi_s$. Assuming that the scattering from the rough surface and vegetation canopy are independent, Equation A1 can be rewritten as

$$T_q = \left\{1 - (W_q^{spec} + W_{q,s}^{diff} + W_{q,v}^{diff})\right\} T \tag{A4}$$

where $W_{q,s}{}^{diff}$ and $W_{q,v}{}^{diff}$ denote diffused albedos from the surface and vegetation respectively. More details about the emission model can be found in Chauhan *et al*. (1994).

The model shown above gives excellent results and has been validated by the author and coworkers for a variety of land covers such as corn, grass and forest (Chauhan *et al*., 1994; Saatchi *et al*., 1994; Chauhan *et al*., 1999b). The model is difficult to invert because of the presence of diffused scattering terms from rough surface and vegetation. However, the model can be simplified and thus invertible if the diffused albedo W^{diff}, is assumed to be negligibly small because of surface and vegetation,. This condition can be satisfied if the terrain is lightly vegetated and/or has low surface roughness conditions. Therefore, Equation A1 is simplified as

$$T_q = T(1 - \left|R_g^q\right|^2\ e^{-2\tau_q} e^{-4k_o^2 s^2 \cos^2\theta_i}) \tag{A5}$$

This equation is identical to Equation 3 shown earlier in Section 3.3. In the above equation $\left|R_g^q\right|^2 = \Gamma_{sq}\Gamma_{iq}^{*}$. A detailed comparison of the Peake's model with the simplified radiative transfer model is discussed in Chauhan (1999a).

It is assumed in Equation A1 that the atmospheric and sky contributions to T_q are small and are ignored here. Microwave brightness temperatures from space are modified by atmosphere. Short-

term comparisons of T_B are generally valid at low frequencies; however, over longer periods (seasonal or yearly) it is necessary to take atmosphere into account. As noted by Choudhury (1993), the magnitude of the effect of atmosphere at mid-latitudes at 19 GHz is of the order of +3K. CMIS frequency used for the soil moisture retrieval process for NPOESS is likely to be lower than 19 GHz. As a result, atmospheric contribution to brightness temperature will be small and is not included here.

The forward model discussed above generates microwave brightness temperature for a particular land surface. The threshold requirement is to estimate soil moisture from bare surfaces. For a smooth bare surface, the horizontal and vertical microwave brightness temperatures are calculated as a function of view angle and soil moisture (Equation A4). Microwave response from a rough surface is generated by including both coherent and incoherent reflectives (Equations A2 and A3). We have used Kirchhoff's model to represent a rough surface having RMS height=3 cm and correlation length=10 cm. Incoherent reflectivity is included using Peake's approach (Chauhan *et al.*, 1994). The radiometer/model response for a smooth and rough surface at a frequency of 6 GHz (a probable CMIS frequency) is shown in Figure A2. The results of the forward model shown here are for volumetric soil moisture of 20 percent. The model discussed here represents the state of the art, and their forward and inverse results have been validated against a number of experimental data sets (Chauhan, 1997; O'Neill *et al.*, 1996; references therein). The data sets produced by the forward models are inverted using the method discussed in Section 3.3.2.1, and the results are compared with the input/actual soil moisture for both smooth, rough bare and weakly vegetated surfaces.

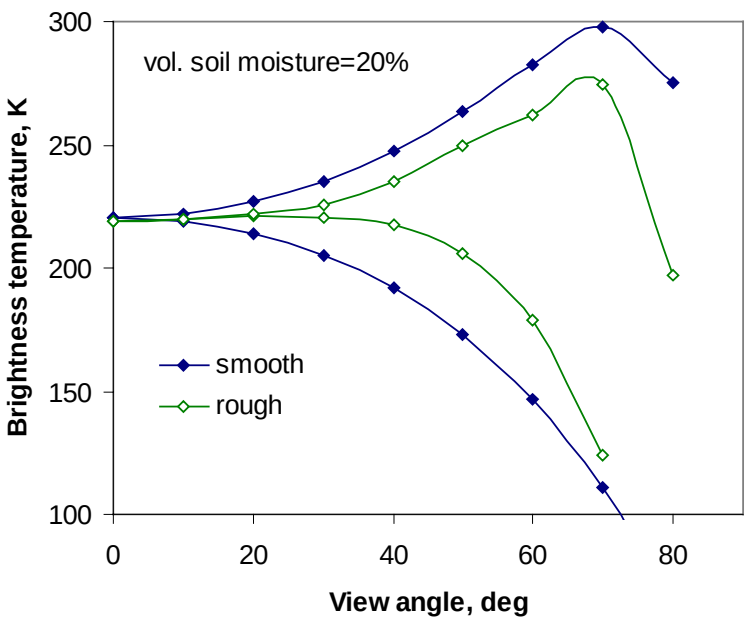

Figure A2. Forward model for smooth and rough (s=3 cm l=10cm) surface without vegetation cover.

Most of the past studies have used horizontal polarization data for the inversion of soil moisture. This however requires *a priori* information about the surface roughness and this information is not available on a global basis. If surface roughness correction is not applied to data then the inversion results are not correct. This is shown in Figure A3, where the forward model is inverted using both single polarization and dual polarization technique. As noticed from Figure A3, the dual polarization results are much better than single polarization results. Note that for the flat surface, the choice of polarization inversion technique is not important.

Data from operational sensors are often corrupted by noise; therefore, the forward model data set needs to be corrupted with noise prior to inversion in order to mimic a realistic retrieval of soil moisture. To test the present soil moisture estimation algorithm against such conditions, we have corrupted the brightness temperature obtained from the model with varying degrees of random noise. The results of the inversion are shown in Figure A4. The inversion process is robust and gives results well within the acceptable noise level of microwave sensors. At present, we do not know the noise level of CMIS; therefore exact evaluation of noisy data cannot be performed. For SSM/I sensor NEDT is less than 0.5K.

Retrieval of soil moisture from surfaces other than bare soils, (e.g., vegetated surfaces) is an "objective" requirement of NPOESS. In the case of soil moisture, this objective is an active area of research. Therefore, retrieval of soil moisture from vegetated surfaces will evolve with time. A brief summary of our plans and some preliminary results are given here. A look at Equation 1 reveals that two vegetation parameters, i.e., single-scattering albedo and optical depth, are required for the vegetated surface. If some vegetation characteristics are known, then these two parameters can be calculated using a discrete scatter model of a particular vegetation canopy (Chauhan *et al.*, 1994). Either LAI or NDVI information can be used to calculate vegetation optical depth and/or scattering albedo. The approach is quite involved and will not be discussed in the current version of the ATBD. Here, soil moisture retrievals using dual-polarization inversion technique are used. For details including the sensitivity studies using this technique, see Section 3.4. The results are discussed for a canopy of soybean that has an LAI of 3.

To summarize, the application of the retrieval algorithm to model data yields reasonably accurate soil moisture results. The retrieval technique is robust enough to handle experimental noise and weakly vegetated areas. The results from the forward model and the inverse problem were validated earlier against experimental data for low (L-band) microwave frequency (Chauhan, 1997; Chauhan *et al.*, 1994; O'Neill *et al.*, 1996).

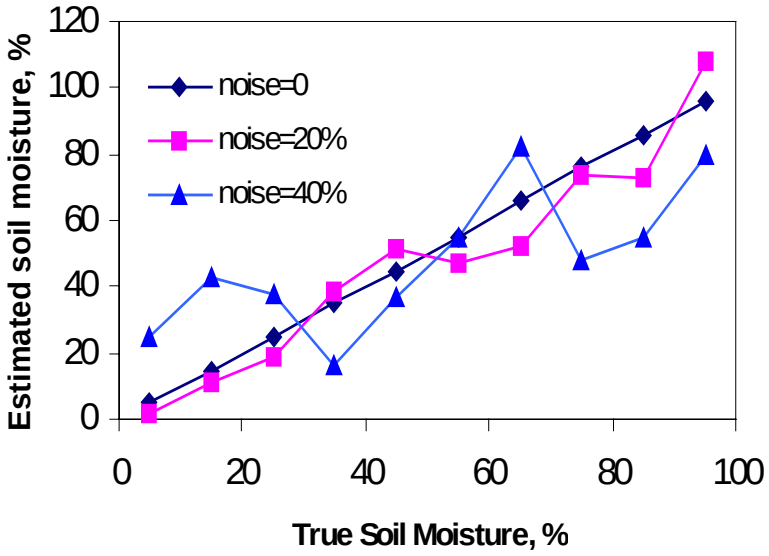

Figure A3. Microwave estimates of soil moisture from bare (rough and flat) surfaces using single polarization and dual-polarization inversion techniques.

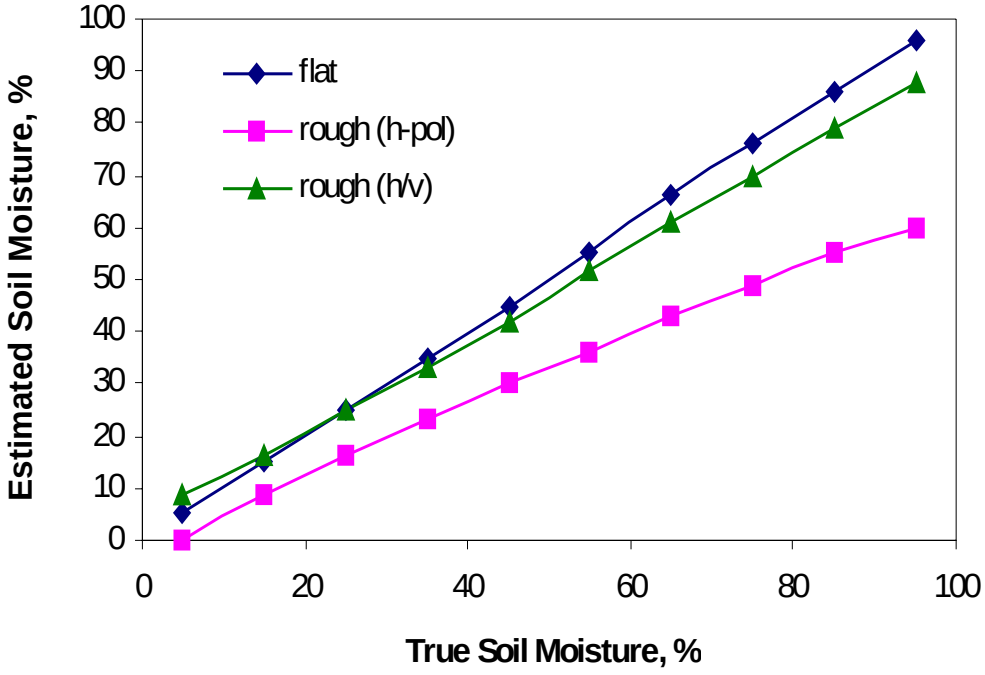

Figure A4. Illustration of robustness of the soil moisture inversion against noisy data.